FLOW ASSURANCE: DROP AND BUBBLE COALESCENCE AND THIN FILM RUPTURE*

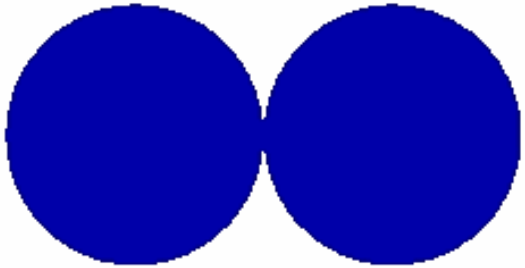

Osman A. Basaran and Vishrut Garg

Purdue Process Safety and Assurance Center (P2SAC)

Davidson School of Chemical Engineering

Purdue University

W. Lafayette, IN 47907, USA

obasaran@purdue.edu

**With special thanks to Krish Sambath (now at Chevron) and Sumeet Thete (now at Air Products)*

Examples of flow assurance

- Coalescers, dehydrators, desalters, and oil-water separators (widely used in the oil & gas industry)*
- Hydrate formation in oil and gas pipelines#
- Spray drift in agriculture*
- "Drop size-modulation" and "satellite droplet or misting prevention" in ink jet printing and other drop-wise manufacturing or printing operations*
- Rupture of coated thin films on substrates*
- Rupture of free thin films/sheets (important in atomization and polymer processing)*

---

*Studied in the Basaran group

Studied in the Corti and Franses groups

Electrostatic coalescers (dehydrators/desalters)

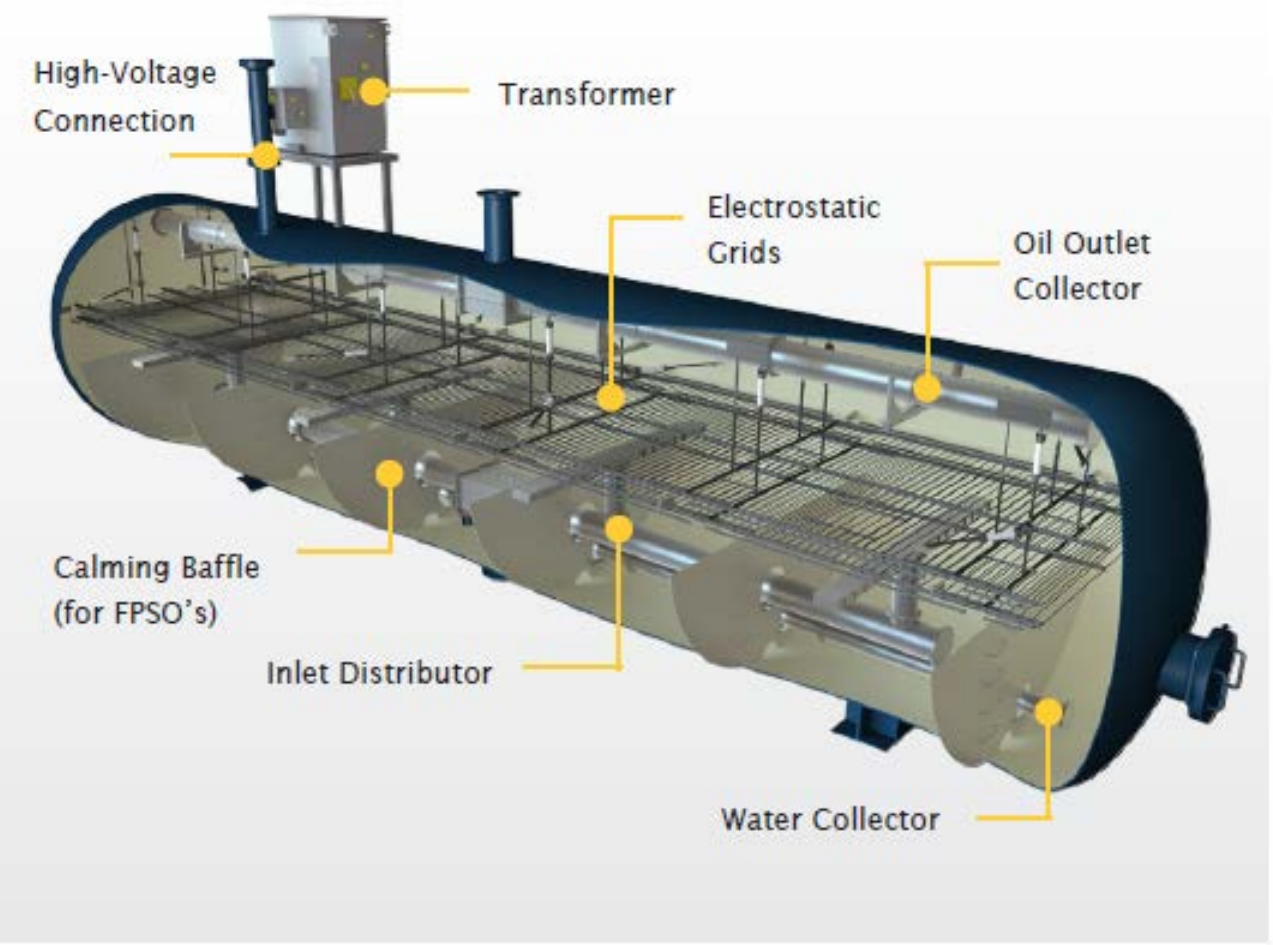

3D model of Frames Electrostatic Coalescer

Frames
Separation Technologies
Glazenmakersweg 3
3449 JK Woerden
The Netherlands

+31 88 00 333 00
separation@frames-group.com
frames-group.com

FRAMES
a family of oil & gas solutions

Electrostatic Coalescers (Dehydrators / Desalters)

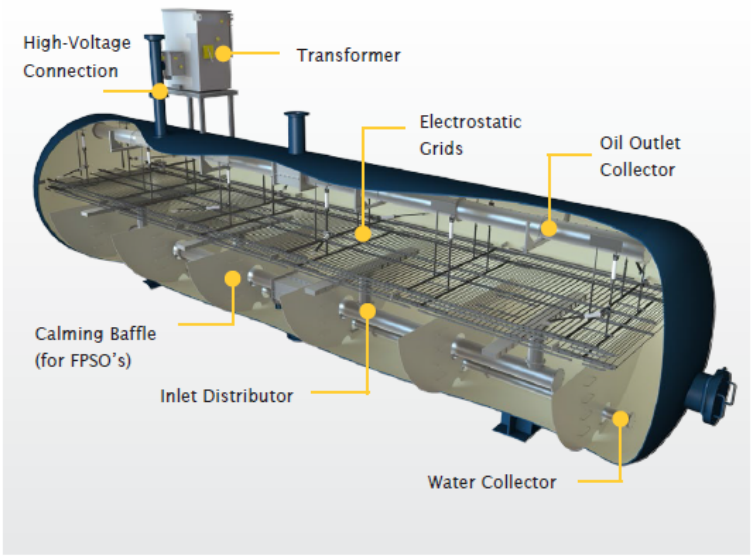

3D model of Frames Electrostatic Coalescer

Product Definition

Frames' proprietary electrostatic coalescers are 2-phase separators that utilize an electrostatic field to remove water and salts from crude oil, allowing cost-effective transport and protect downstream processes.

Dehydration

In the process of removing water from oil, electrostatic treatment is typically preceded by 2-phase or 3-phase bulk separation in the upstream process. Electrostatic coalescers are applied as the final separation step to break up emulsions and reduce the remaining water fraction (dehydration). This is the reason why they are typically applied in upstream applications.

Desalting

Electrostatic coalescers are also applied for desalting in order to reduce the crude's salt content. Because salts are soluble in water, a reduction in water fraction will automatically reduce the crude's salt content. Desalting therefore often occurs in two stages: the first stage (dehydration) is followed by a second stage (desalting), where the salts are diluted by the addition of wash water between the first coalescer (dehydrator) and the second (desalter). The main aim of having a second stage in the system is to ensure a high dilution rate (ratio of wash water and water fraction in the crude). This dilution is necessary since dehydration alone is usually not sufficient to reach typical salinity values in the export crude (~10 - 100 PTB).

Frames
Separation Technologies
Glazenmakersweg 3
3449 JK Woerden
The Netherlands

+31 88 00 333 00
separation@frames-group.com
frames-group.com

FRAMES
a family of oil & gas solutions

Process Description

Frames builds on its vast experience in coalescer engineering, enabling us to give our clients a competitive advantage when it comes to cleaning crude oil. By efficiently and effectively removing undesirable water and salts, our clients are able to increase the quality of their crude oil, cut their transport costs and protect their downstream processes and equipment.

Removal of water and contaminants generally comprises two steps: dehydration and desalting. Frames coalescers are designed for both steps, and are applied in upstream as well as downstream applications. In oilfields, the emphasis is generally on a combination of dehydration and desalting, whereas in refineries the focus is primarily on desalting.

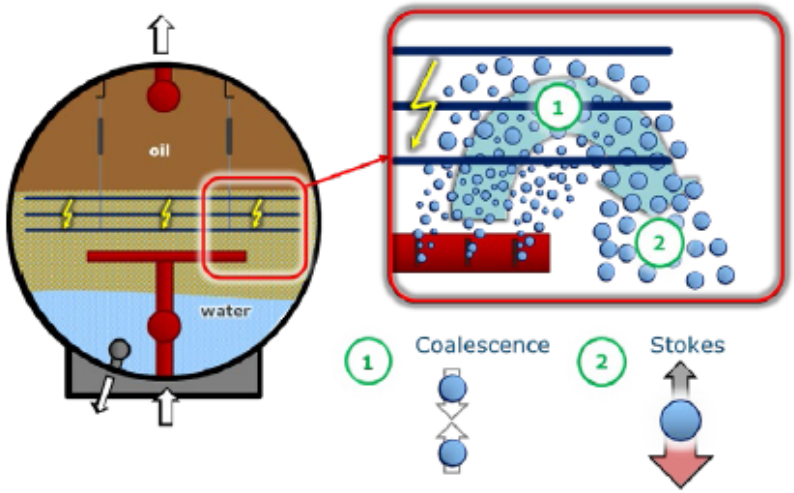

Working principle of coalescence (1) and separation (2) inside Electrostatic Coalescer

Frames
Separation Technologies
Glazenmakersweg 3
3449 JK Woerden
The Netherlands

+31 88 00 333 00
separation@frames-group.com
frames-group.com

FRAMES
a family of oil & gas solutions

Common features of all the flow assurance problems under consideration

Breakup and coalescence problems all involve:

- **Hydrodynamic singularities (technical name: finite time singularities)**
- **Free surface flows involving topological changes**
- **Disparate length scales (multi-scale physics), e.g. if the initial drop size is 1 mm and at "breakup" the thread radius is 10 nm (the limit of continuum mechanics), *length scales differing by 5 orders of magnitude or a factor of* 10^5 *must be resolved in a single simulation!!! (Commercial codes/diffuse interface methods can barely do 2 orders.)***

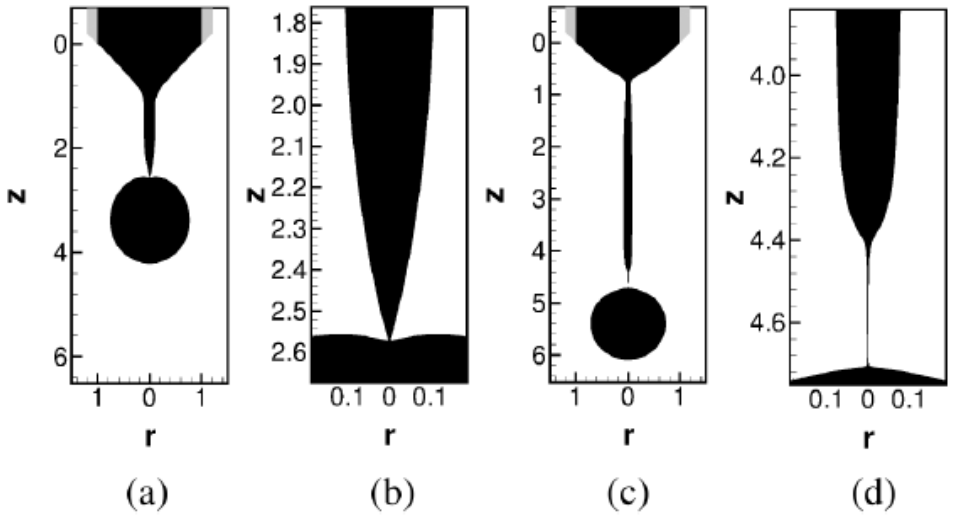

FIG. 1. Computed shapes of water, (a),(b), and 83% glycerol, (c),(d), drops at the incipience of pinch-off. Here (a) and (c) show the global shapes and (b) and (d) show their blowups in the vicinity of $h_{\min}$. For the water drop, $h_{\min} = 2 \times 10^{-3}$, and for the 83% glycerol drop, $h_{\min} = 1 \times 10^{-3}$.

Major award from the American Physical Society's Division of Fluid Dynamics (largest and most important organization of engineers/scientists working in fluid dynamics)

2017 Stanley Corrsin Award

To recognize and encourage a particularly influential contribution to fundamental fluid dynamics.

Jens Eggers
University of Bristol
Citation:

"For analysis of **singularities** as a unifying theme for physical and mathematical insights into a wide variety of two-phase fluid mechanics problems involving **jets**, **coalescence**, entrainment and wetting."

IOP Publishing Reports on Progress in Physics
Rep. Prog. Phys. **71** (2008) 036601 (79pp) doi:10.1088/0034-4885/71/3/036601

Physics of liquid jets

Jens Eggers[1] **and Emmanuel Villermaux**[2,3]

[1] School of Mathematics, University of Bristol, University Walk, Bristol BS8 1TW, UK
[2] IRPHE, Université de Provence, Aix-Marseille I, Technopôle de Château-Gombert, 49, rue Frédéric Joliot-Curie 13384 Marseille Cedex 13, France

"Top" "Bottom"

Figure 3. (Top) Sprays produced by jets are widely used in agricultural irrigation. The big drops from the rupture of the jet fall rapidly on the ground where they may damage the plants while smaller ones go with the wind, possibly across the field and farther, causing a loss of water, or pesticide. Controlling the drop size distribution remains a crucial issue in this context. (Bottom) The 'Bosquet des Trois Fontaines' in Le Nôtre's Versailles garden (1677). Engraving by Jean Rigaud.

- **Spray drift due to small drops**
- **Avoidance of production of small drops: prevention through design! (Active area of research in the group.)**

Flow assurance: spray drift example from crop spraying or crop protection

A liquid sheet from a fan spray nozzle (Crapper et al. JFM 1973; Villermaux ARFM 2007)

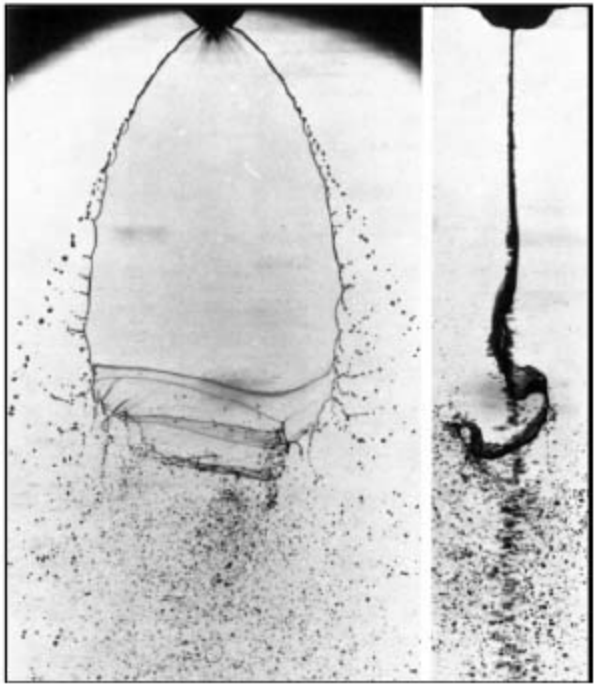

Small drops are undesirable because they lead to drift

Spray drift is the most common cause of off-target movement of chemicals (e.g. pesticides) in crop spraying. It can injure or damage plants, animals, the environment or property, and even affect human health. “Drift” is the airborne movement of agricultural chemicals as droplets, particles or vapor.

Nonstandard Inkjets

Annu. Rev. Fluid Mech. 2013. 45:85–113

Osman A. Basaran,[1] Haijing Gao,[1,2] and Pradeep P. Bhat[1,3]

[1]School of Chemical Engineering, Purdue University, West Lafayette, Indiana 47906; email: obasaran@purdue.edu

[2]Advanced Production Systems, Chevron Energy Technology Company, Houston, Texas 77002; email: Haijing.Gao@chevron.com

[3]3M Display and Graphics Film Lab, 3M Company, St. Paul, Minnesota 55144; email: ppbhat@mmm.com

Squeeze-mode piezo sleeve and 35 µm glass nozzle used in DNA microarraying and other cutting edge applications

"Standard" waveform and big drops (plus *undesirable satellites*!)

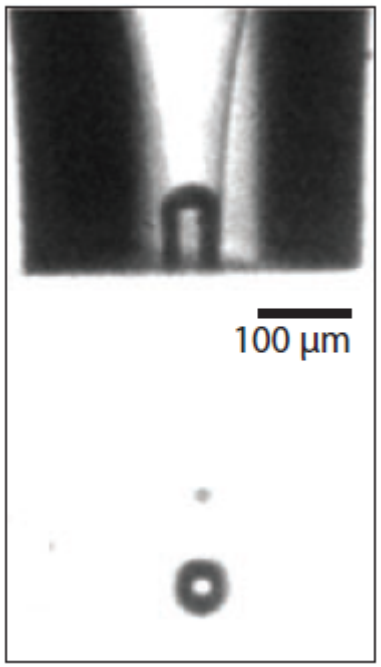

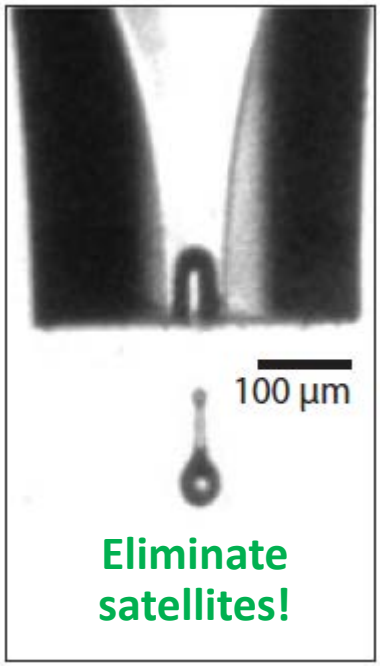

Eliminate satellites!

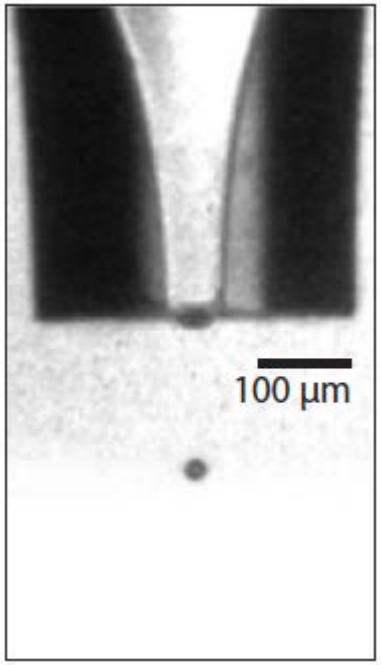

"Novel" waveform and small drops (we can use nozzles from a 1984 HP Thinkjet to make drops as small as is possible today)

Drop size modulation in DOD ink jet printing

Traditidional/standard square wave: "squeeze" (actually, squeeze, hold, and relax) nozzle and "push" liquid out

Non-standard waveform: "suck" and then "push"

Novel (Purdue patented) waveform: "suck", then "push", and finally "suck" again

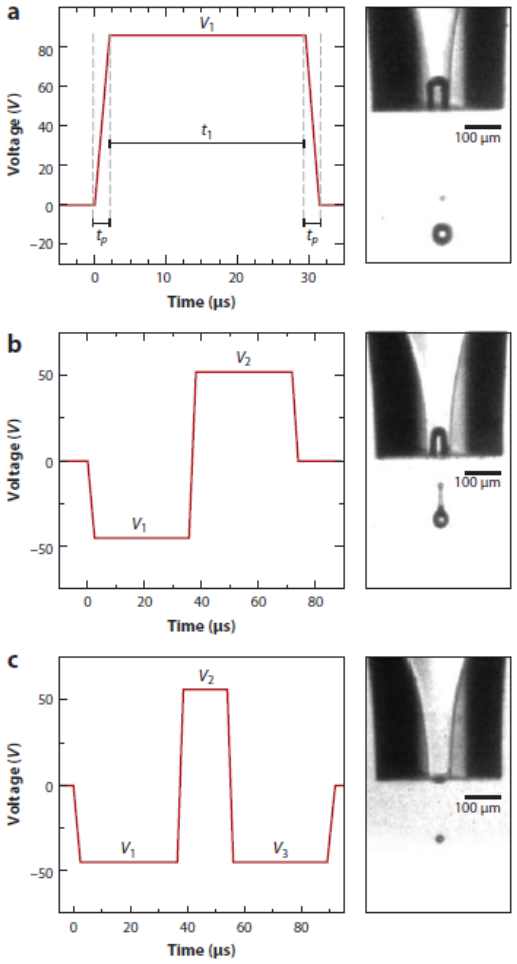

- **Use fluid dynamical understanding (combination of theory, simulation, and ultra high-speed visualization), rather than expensive improvements in manufacturing including production of nozzles of ever smaller radii, to control drop size and eliminate satellites/ fines by using "large" nozzles without risking plugging of "small" nozzles**
- **Purdue 2000-2010: reduced drop radius by a factor of 3-5**
- **Purdue 2010-today: reduced drop radius by a factor of 10-100 (drops you cannot even see!)**

Figure 7

Modulation of drop sizes by driving a piezoelectrically actuated drop-on-demand inkjet nozzle with different drive waveforms. (*a*) For waveform 1, in addition to the large primary drop with size similar to that of the nozzle of $R = 35$ μm, a small satellite droplet is also formed. (*b*) For waveform 2, no satellite is formed, and the drop radius is 42 μm. (*c*) For waveform 3, the drop radius reduces from 42 μm in panel *b* to 16 μm. Thus the radius of the small drop is one-half of the radius of the nozzle.

DOD ink jets: FEM simulations

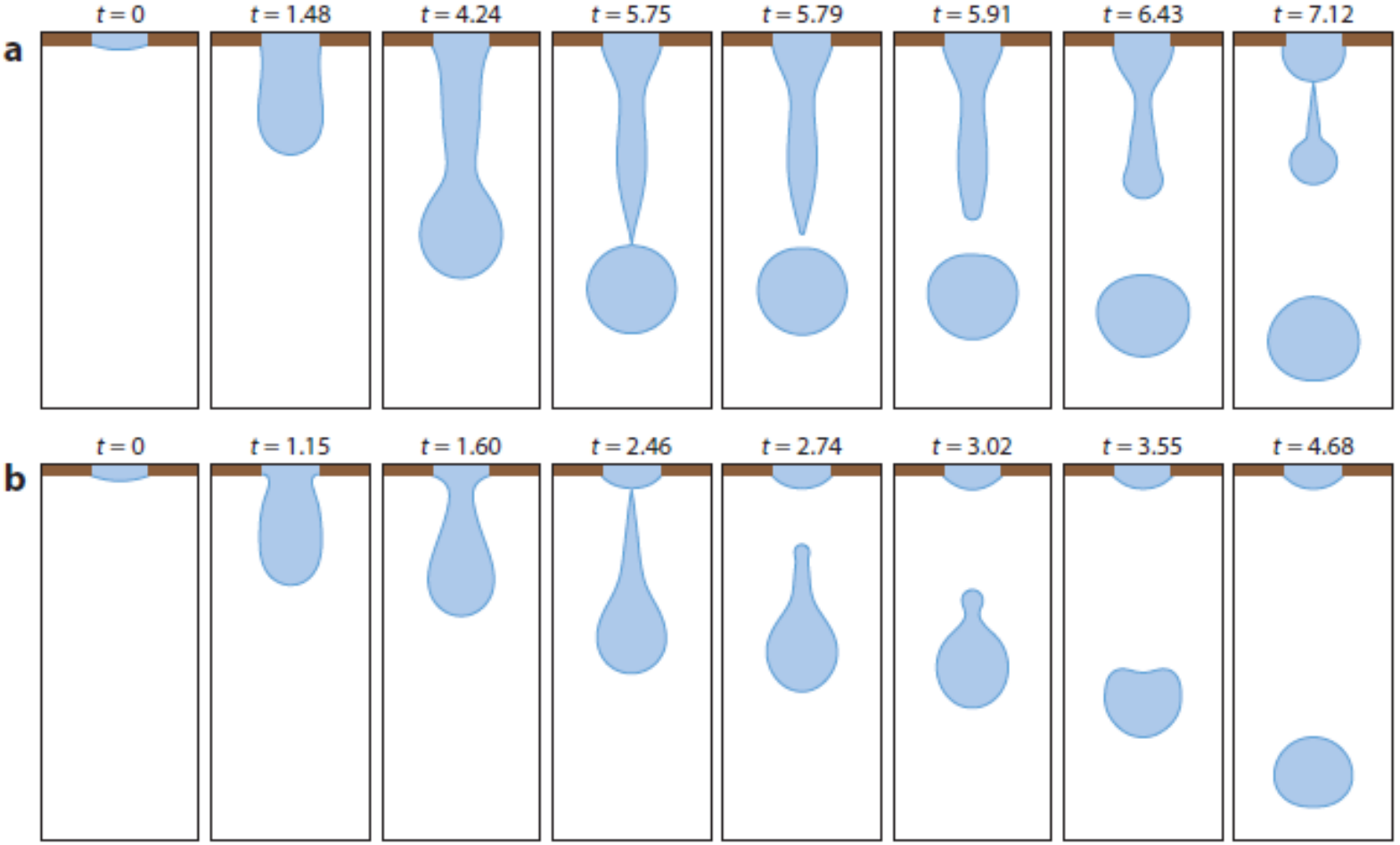

Figure 13

Simulation of drop-on-demand inkjet drop formation driven by a square wave. The algorithm is based on the finite-element method and the elliptic mesh–generation technique. (*a*) Maximum dimensionless injection flow rate We $= 5$, dimensionless pulse width $t_1 = 1$, and duration of falling edge $t_p = 3$. A satellite drop is formed during the recoil of the thread toward the nozzle. (*b*) Maximum dimensionless injection flow rate We $= 7.5$, and dimensionless pulse width $t_1 = 1$. Compared with panel *a*, increasing the injection flow rate can suppress the formation of a satellite drop. In both panels, the characteristic time unit $t_c = \sqrt{\rho R^3/\sigma}$. For a water drop forming from a nozzle of 50 μm, one time unit $t_c = 40\ \mu s$.

J. Fluid Mech. (2017), *vol.* 826, *pp.* 455–483.
doi:10.1017/jfm.2017.446

Critical flow assurance problem in thin film coatings industry, froth floatation, heat transfer, and tear films (dry-eye syndrome)

Self-similar rupture of thin films of power-law fluids on a substrate

Vishrut Garg[1], Pritish M. Kamat[1], Christopher R. Anthony[1], Sumeet S. Thete[1] and Osman A. Basaran[1,†]

[1]School of Chemical Engineering, Purdue University, West Lafayette, IN 47907-1283, USA

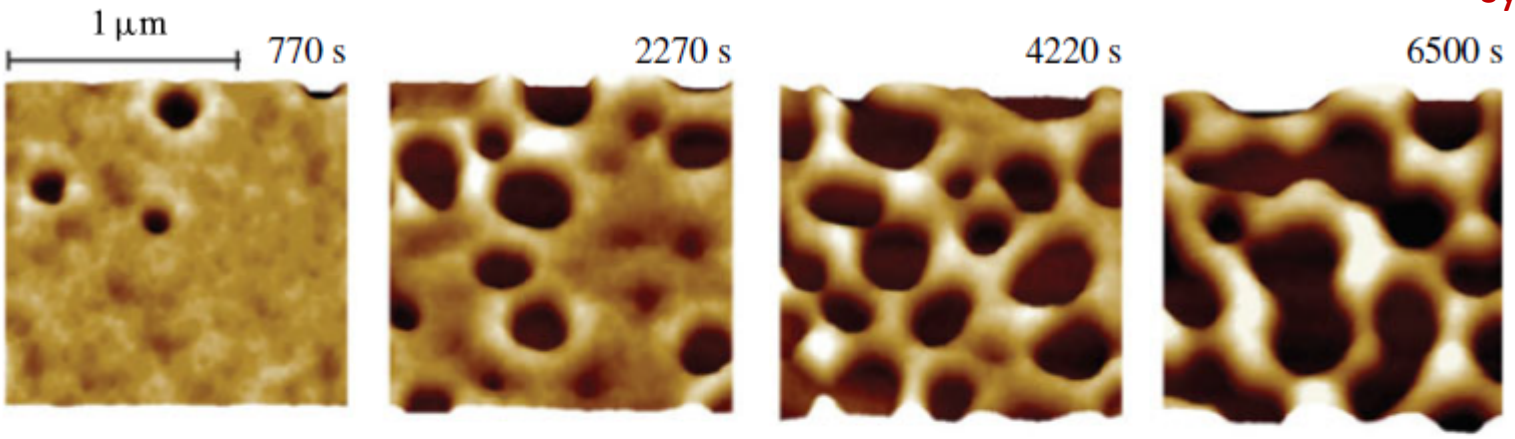

FIGURE 1. (Colour online) Temporal series of AFM scans recorded experimentally showing rupture of a 3.9 nm PS film on an oxidized Si wafer. For this system, the values of the Hamaker constant, surface tension and viscosity are 2.2×10^{-20} J, 30.8 mN m^{-1} and 12 000 Pa s. The scale bar that is shown above the leftmost image applies to all four images. Adapted by permission from Macmillan Publishers Ltd: *Nature Materials* (Becker *et al.* 2003), copyright 2003.

J. Fluid Mech. (2017), vol. 826, pp. 455–483. doi:10.1017/jfm.2017.446

Self-similar rupture of thin films of power-law fluids on a substrate

Vishrut Garg[1], Pritish M. Kamat[1], Christopher R. Anthony[1], Sumeet S. Thete[1] and Osman A. Basaran[1,†]

[1]School of Chemical Engineering, Purdue University, West Lafayette, IN 47907-1283, USA

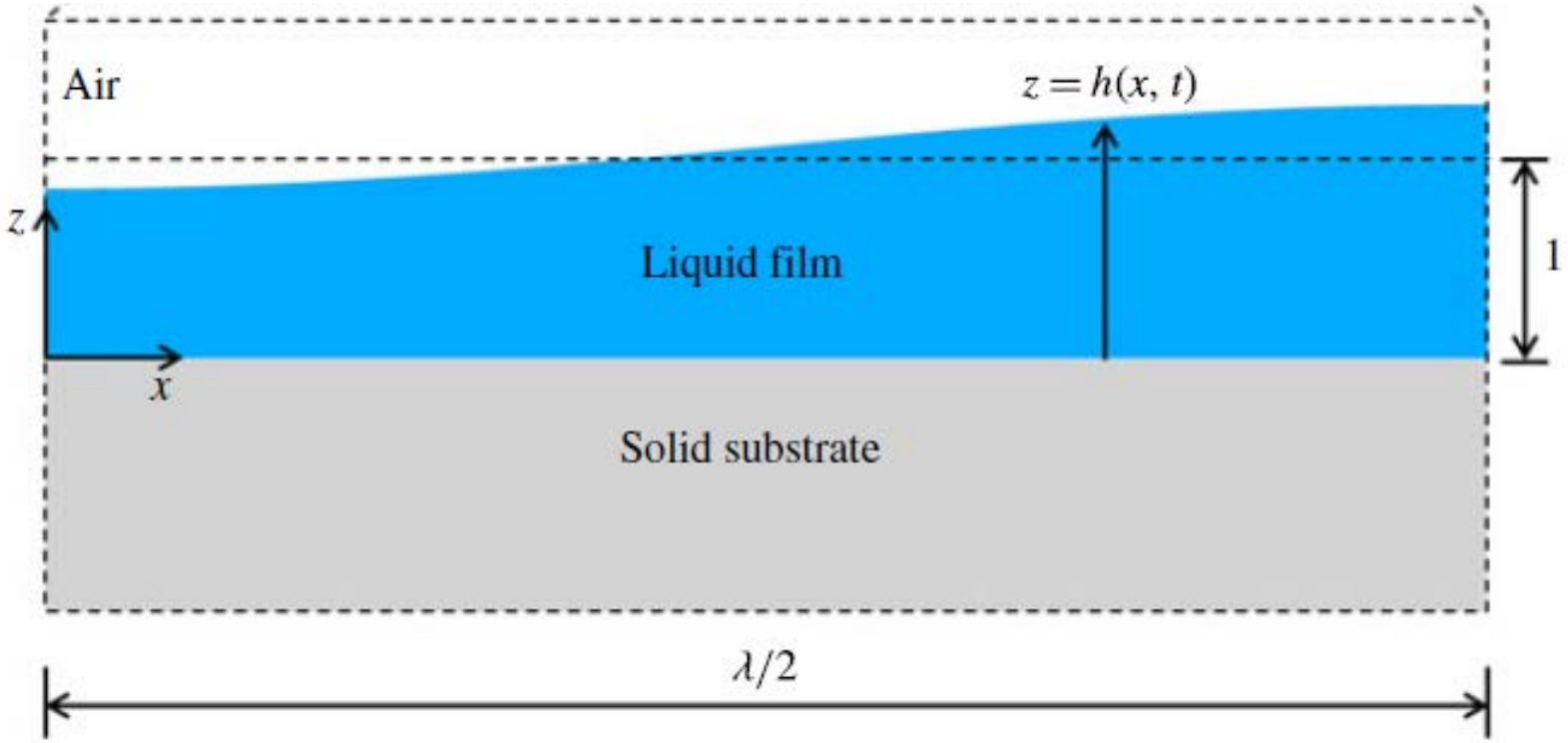

Recent work from our group on rupture of thin free films or liquid sheets

PHYSICAL REVIEW E **92**, 023014 (2015)

Self-similar rupture of thin free films of power-law fluids

Sumeet Suresh Thete, Christopher Anthony, and Osman A. Basaran*
School of Chemical Engineering, Purdue University, West Lafayette, Indiana 47906, USA

Pankaj Doshi
Chemical Engineering and Process Development, National Chemical Laboratory, Pune, India
(Received 28 April 2015; published 12 August 2015)

The rupture of a thin free film of a power-law fluid under the competing influences of destabilizing van der Waals pressure and stabilizing surface tension pressure is analyzed. In such a fluid, viscosity decreases with the deformation rate raised to the $n-1$ power where $0 < n \leqslant 1$ ($n = 1$ for a Newtonian fluid). When $6/7 < n \leqslant 1$, film rupture occurs under a balance between van der Waals pressure, inertial stress, and viscous stress. When $n < 6/7$, however, the dominant balance changes: Viscous stress becomes negligible and the film ruptures under the competition between van der Waals pressure, inertial stress, and surface tension pressure.

More recent work from our group on rupture of thin free films or liquid sheets

PHYSICS OF FLUIDS **28**, 092101 (2016)

Self-similarity and scaling transitions during rupture of thin free films of Newtonian fluids

Sumeet Suresh Thete,[1] Christopher Anthony,[1] Pankaj Doshi,[2]
Michael T. Harris,[1] and Osman A. Basaran[1,a)]
[1]*School of Chemical Engineering, Purdue University, West Lafayette, Indiana 47907, USA*
[2]*Pfizer Worldwide R&D, Groton, Connecticut 06340, USA*

(Received 20 June 2016; accepted 11 August 2016; published online 6 September 2016)

Rupture of thin liquid films is crucial in many industrial applications and nature such as foam stability in oil-gas separation units, coating flows, polymer processing, and tear films in the eye. In some of these situations, a liquid film may have two free surfaces (referred to here as a free film or a sheet) as opposed to a film deposited on a solid substrate that has one free surface. The rupture of such a free film or a sheet of a Newtonian fluid is analyzed under the competing influences of inertia, viscous stress, van der Waals pressure, and capillary pressure by solving a system of spatially one-dimensional evolution equations for film thickness and lateral velocity. The dynamics close to the space-time singularity where the film ruptures is asymptotically self-similar and, therefore, the problem is also analyzed by reducing the transient partial differential evolution equations to a corresponding set of ordinary differential equations in similarity space. For sheets with negligible inertia, it is shown that the dominant balance of forces involves solely viscous and van der Waals forces, with capillary force remaining negligible throughout the thinning process in a viscous regime. On the other hand, for a sheet of an inviscid fluid for which the effect of viscosity is negligible, it is shown that the dominant balance of forces is between inertial, capillary, and van der Waals forces as the film evolves towards rupture in an inertial regime. Real fluids, however, have finite viscosity. Hence, for real fluids, it is further shown that the viscous and the inertial regimes are only transitory and can only describe the initial thinning dynamics of highly viscous and slightly viscous sheets, respectively. Moreover, regardless of the fluid's viscosity, it is shown that for sheets that initially thin in either of these two regimes, their dynamics transition to a late stage or final inertial-viscous regime in which inertial, viscous, and van der Waals forces balance each other while capillary force remains negligible, in accordance with the results of Vaynblat, Lister, and Witelski. *Published by AIP Publishing.*

Applications of emulsions and coalescence

Oil and gas industry

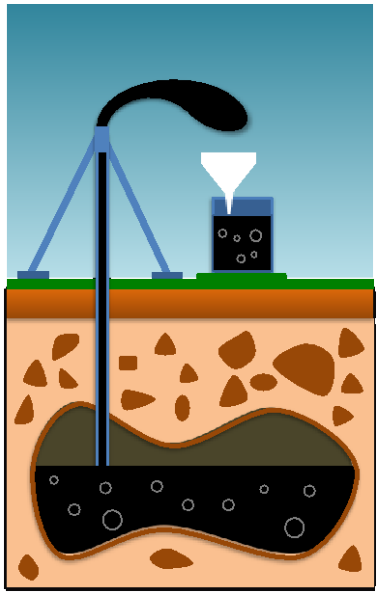

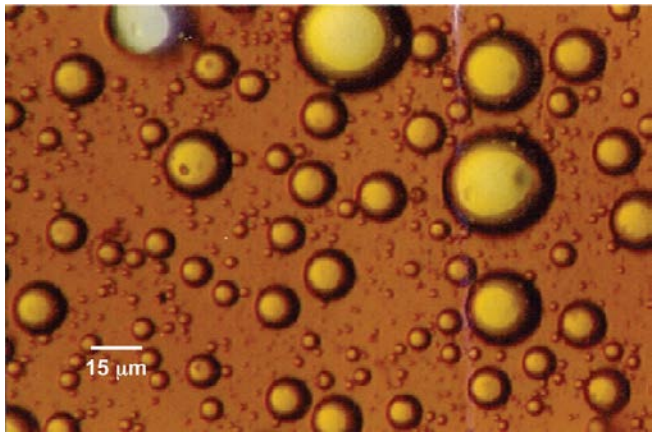

Water-in-oil (W/O) emulsions are common in almost all phases of oil processing and production

Food industry

O/W emulsion

W/O emulsion

Pharmaceuticals

Ointments

Intravenous lipid emulsions

Agriculture

Insecticides are prepared as oil-in-water (O/W) emulsions for cheap and effective application

Making (stabilizing) and breaking emulsions and designing coalescers

- Empiricism, rules of thumb, and other methods not relying on fundamentals
- Experiment
- Molecular dynamics (not yet useful in engineering design)
- Population balances: determine evolution of drop sizes or drop size distributions using semi-empirical models for collision rates of drops and coalescence probabilities
- Analysis of local dynamics of two drop interactions using simulation or computational analysis (the results of which can be fed back into population balance models to make engineering calculations and designs)

TWO DISTINCT COALESCENCE PROBLEMS

Pre-coalescence problem

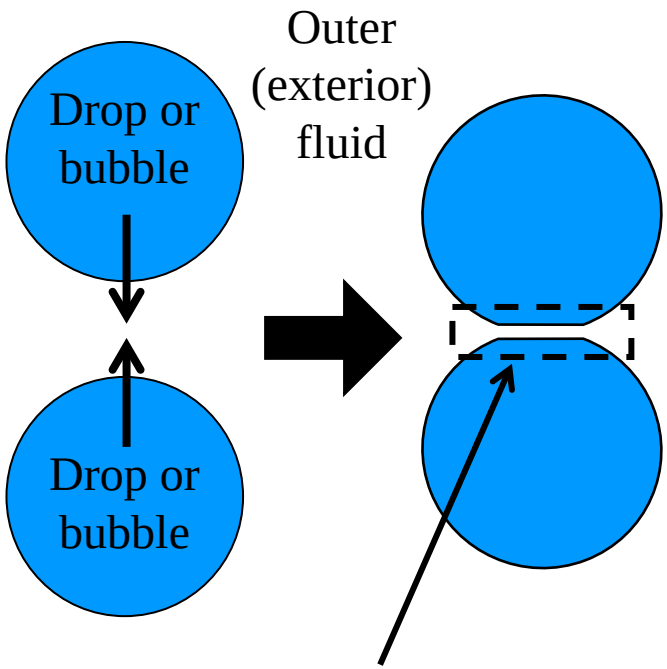

Thin film/sheet (that has to rupture for coalescence to occur)

Singularity at the end of the process

Post-coalescence problem

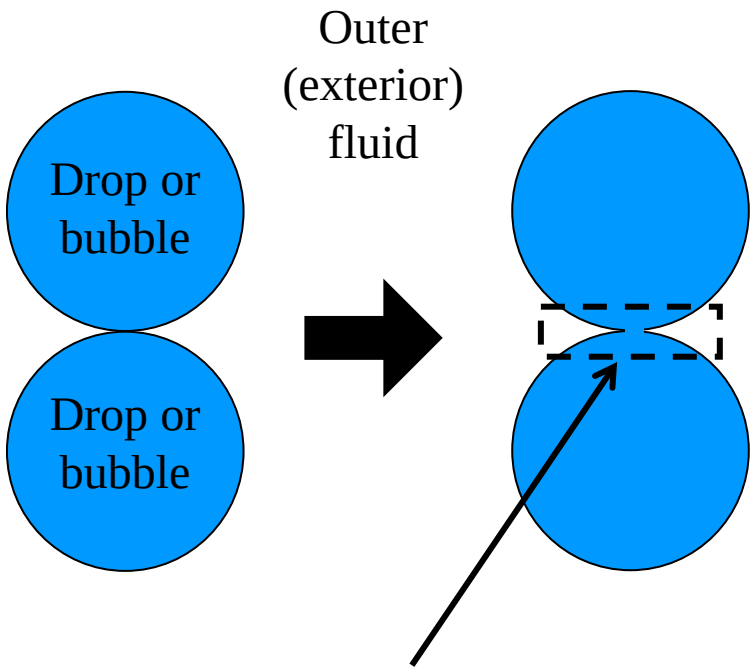

Thin film/sheet with a growing hole (or a growing bridge that connects the two drops/bubbles)

Singularity at the beginning of the process

(Post) Coalescence of liquid drops: process driven by initial singularity in curvature and capillary pressure

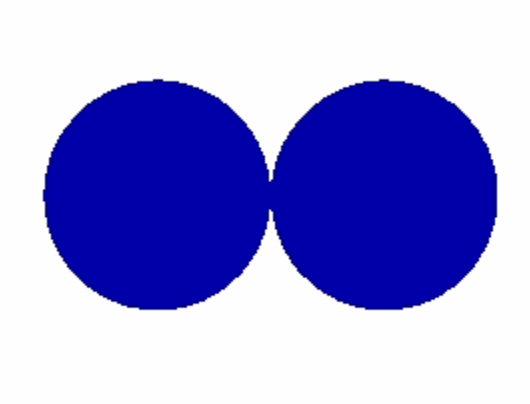

Fluid dynamics of drop pairs: Pre-coalescence problem

Water drops in oil or oil drops in water

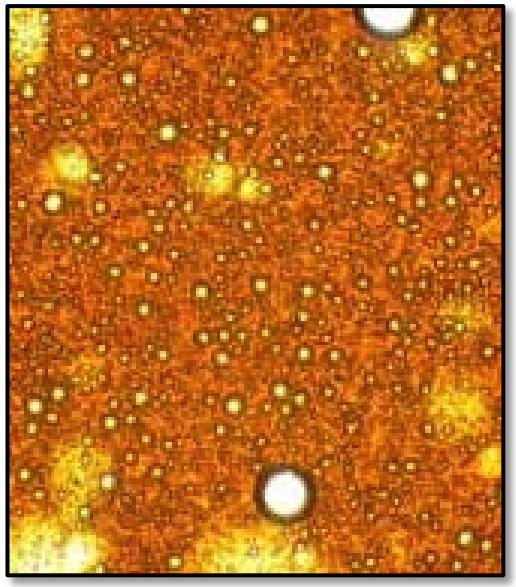

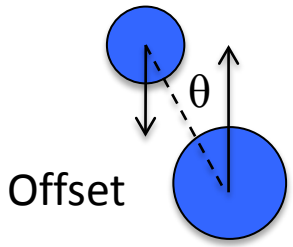

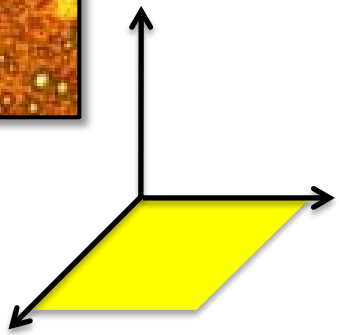

Flow properties

$(R_1, R_2, d_{12}, U_1, U_2)$

Fluid properties

$(\rho_1, \rho_2, \mu_1, \mu_2, \gamma_{12}, A_H)$

Two drops of equal size colliding head on

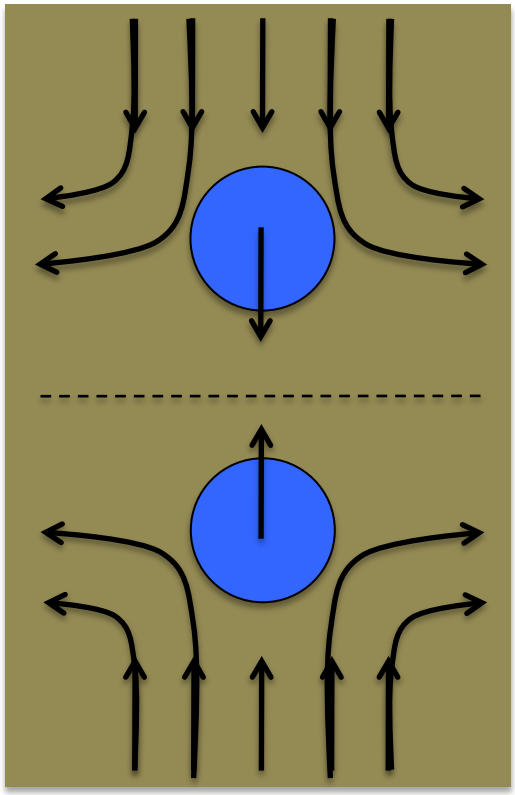

Previous works

All the best studies are restricted to creeping/Stokes flow, i.e. Re=0.

- **R.H. Davis and co-workers** (1990 – 1997)
  - Lubrication approximation
  - Scaling theory
- **L.G. Leal and co-workers** (2001 – present)
  - Experiments using Taylor's four roll mill
  - Boundary integral (BI) simulations
  - Scaling theory
- **M. Loewenberg and co-workers** (2004 – 2010)
  - BI sims (role of internal flows in arresting drop coalescence
- **H. Meijer and co-workers** (2006 – present)
  - Boundary integral simulations
  - Scaling theory

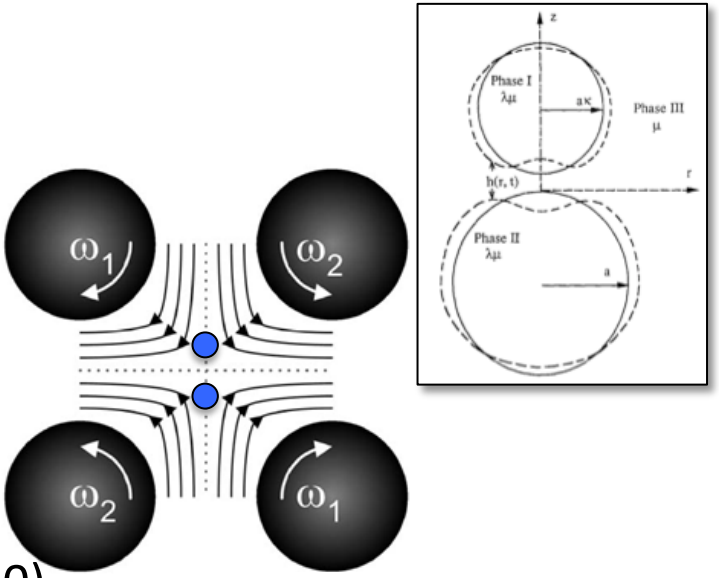

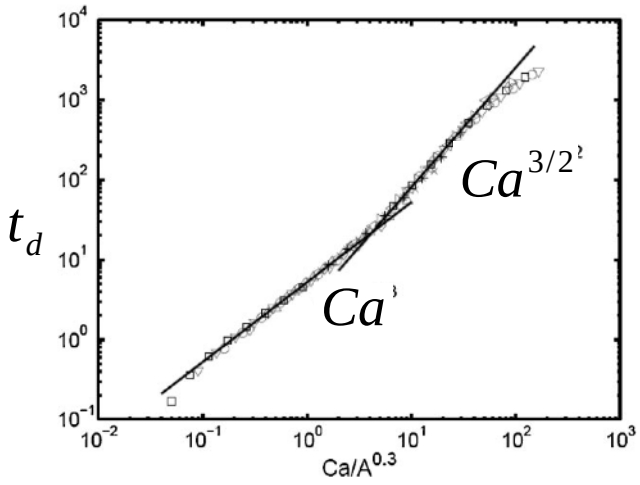

Problem setup

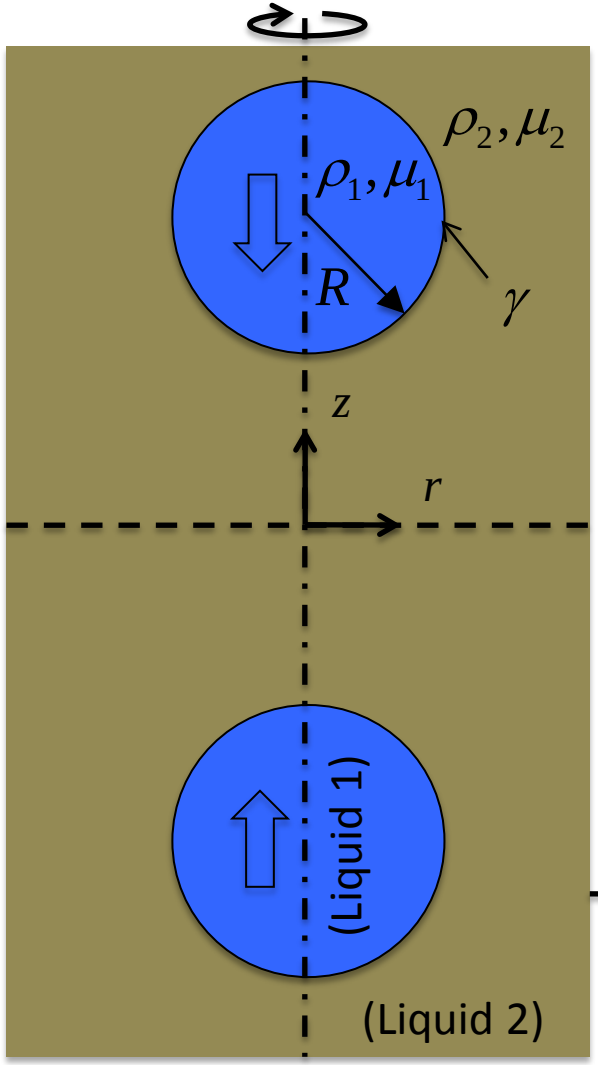

Imposed bi-axial extensional flow

$$\mathbf{u}_0(\mathbf{x}) = G\left(\frac{r}{2}\mathbf{e}_r - z\,\mathbf{e}_z\right)$$

Key Dimensionless groups:		1 mm water drops in oil
$Ca = \dfrac{GR\mu_2}{\gamma}$	Capillary number or viscous / surface tension force	10^{-4} to 0.1
$A^* = \dfrac{A_H}{6\pi\gamma R^2}$	Van der Waals force / Surface tension force	10^{-13}
$m_i = \mu_i / \mu_1 \quad i=1,2$	Viscosity ratio	10
$d_i = \rho_i / \rho_1$	Density ratio	0.9
$Oh = \dfrac{\mu_1}{(\rho_1 R\gamma)^{1/2}}$	Ohnesorge number or dimensionless viscosity	0.006
$Re = \dfrac{GR^2\rho_2}{\mu_2} = \dfrac{Ca\ d_2}{(m_2 Oh)^2}$		0.01 to 10

Different non-dimensionalizations

- Dimensionless external or approach velocity driving the two drops together: $U_\infty = G\sqrt{\rho_1 R^3/\gamma}$ ← Inertial-capillary (Rayleigh) time
- Ca is velocity made dimensionless with viscous-capillary time and U_∞ is that using inertial-capillary time
- Note that $Ca = m_2 Oh U_\infty$. In Stokes flow, $Oh \to \infty$ but $U_\infty \to 0$ so that Ca is finite
- Thus, one possible set of dimensionless groups is: Oh, m_2, d_2, Ca, A^* (Stokes limit is obtained by setting $Oh^{-1} = 0$ and dropping d_2 from the list of dimensionless parameters)
- A second set of candidate dimensionless groups is: $Oh, m_2, d_2, U_\infty, A^*$ (used in the remainder of the talk)

Mathematical formulation

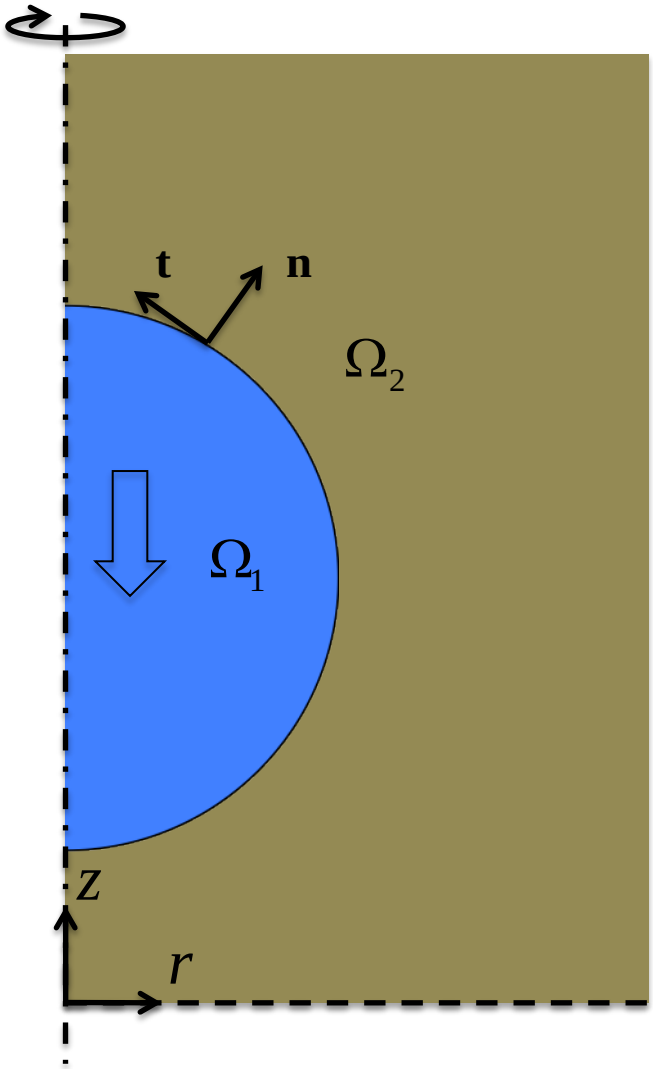

Navier-Stokes system:

$$\left.\begin{aligned} \nabla \cdot \mathbf{v}_i &= 0 \\ d_i\left(\frac{\partial \mathbf{v}_i}{\partial t} + \mathbf{v}_i \cdot \nabla \mathbf{v}_i\right) &= \nabla \cdot \mathbf{T}_i \end{aligned}\right\} \Omega_1 \cup \Omega_2$$

where $\mathbf{T}_i = -p_i \mathbf{I} + m_i Oh\left(\left(\nabla \mathbf{v}_i\right) + \left(\nabla \mathbf{v}_i\right)^T\right)$

Boundary conditions:

$$\left.\begin{aligned} \mathbf{n} \cdot \left(\mathbf{v}_i - \mathbf{v}_{s,i}\right) &= 0 \\ \mathbf{n} \cdot \left[\mathbf{T}_i\right]_1^2 &= \left(2H - \frac{A^*}{h(\mathbf{x})^3}\right)\mathbf{n} \end{aligned}\right\} \partial\Omega_{1-2}$$

where $h(\mathbf{x})$ – vertical separation between drops' interfaces

For typical liquids, $A_H = 10^{-21}$ to $10^{-18}\ J$

Elliptic mesh generation

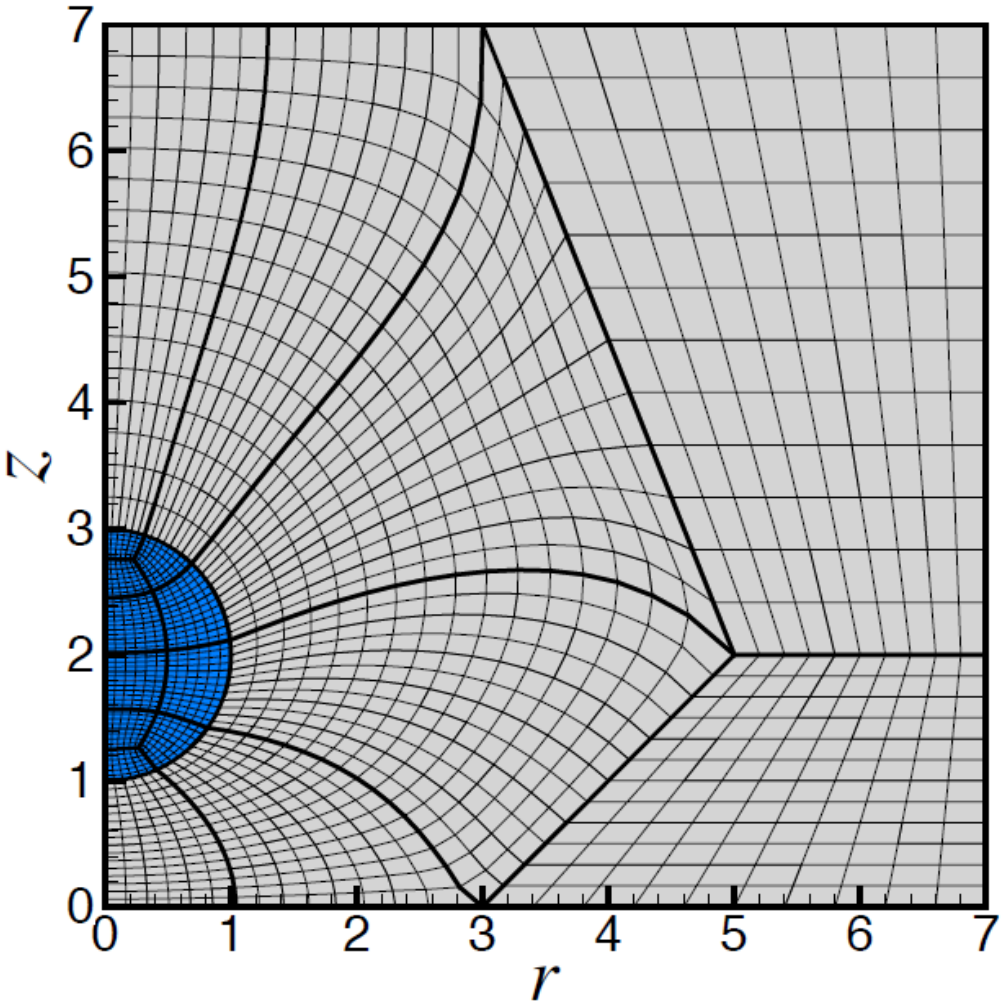

Approach dynamics

$Oh = 0.1,\ \ m_2 = 5.3,\ \ d_2 = 1.1,\ \ U_\infty = 0.0285,\ \ A^* = 5 \times 10^{-11}$

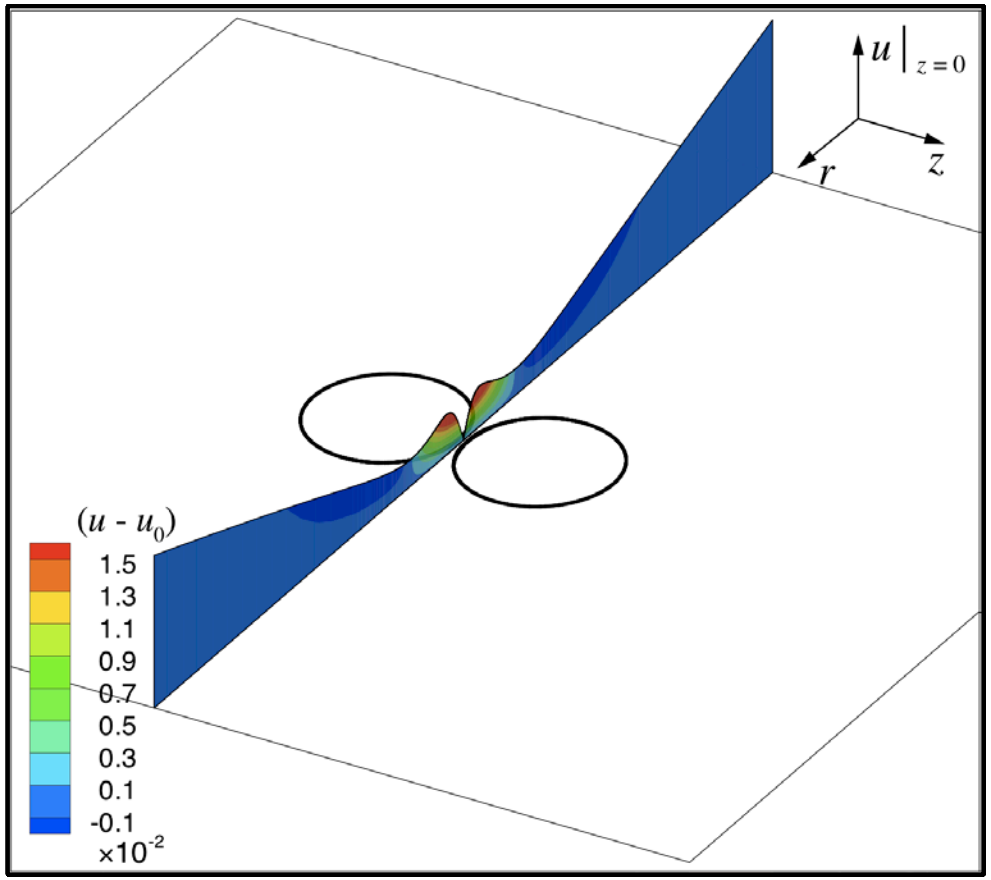

When does film drainage begin?

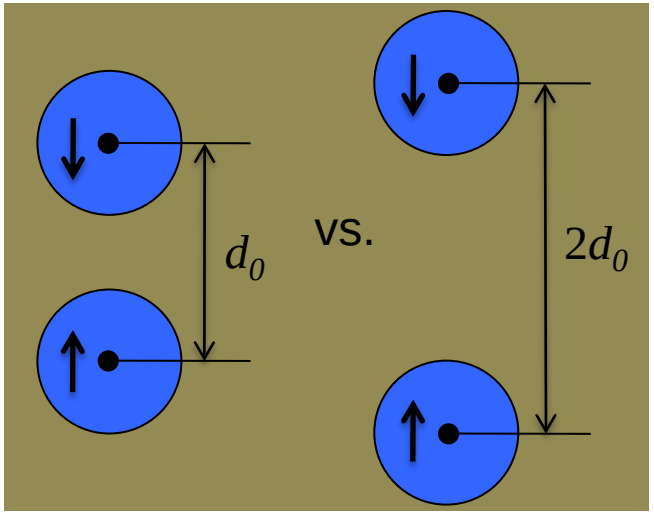

Film drainage is *taken* to **begin** when

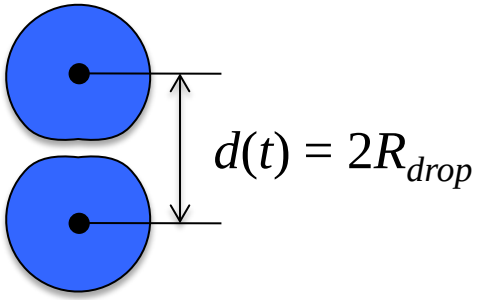

Final stages of film drainage

$Oh = 0.1,\ \ m_2 = 5.3,\ \ d_2 = 1.1,\ \ U_\infty = 0.0285,\ \ A^* = 5 \times 10^{-11}$

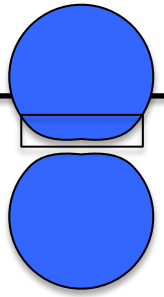

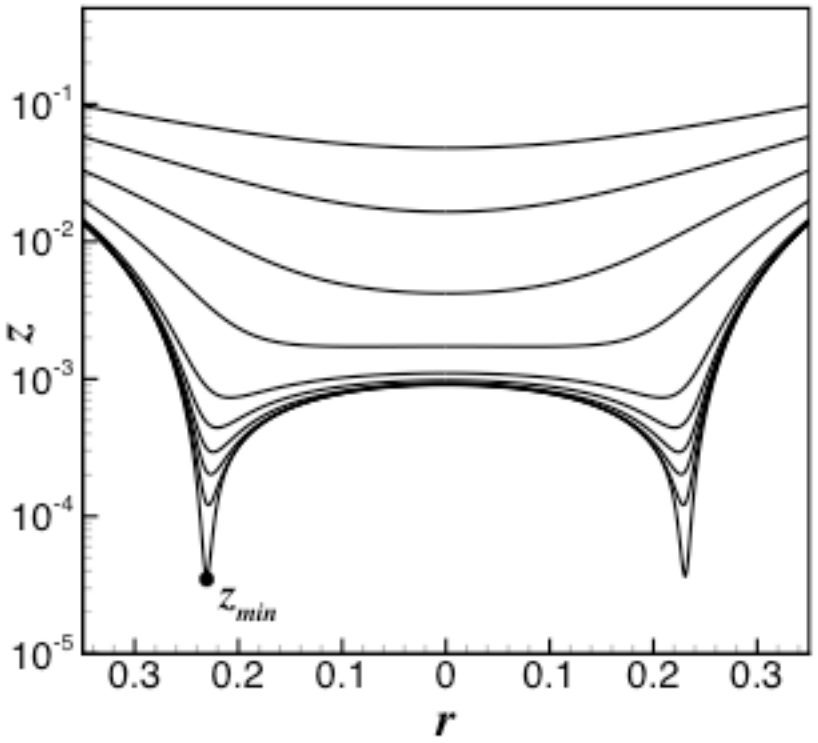

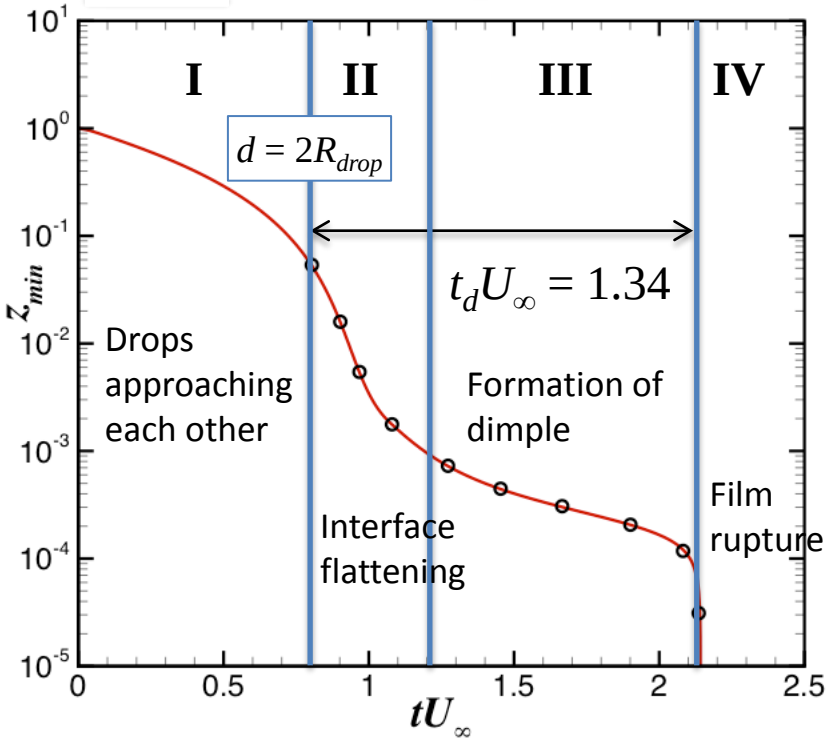

- *Experimentally* measured **drainage time** for 27 μm sized poly-butylene drops coalescing in silicone oil (Yoon *et al.* 2007) } : $t_d U_\infty \approx 1.32$

Drainage time

Previous works:

$$U_\infty = 0.05,\ A^* = 10^{-10},\ d_2 = 1$$

Contradicting reports on scaling laws for drainage time

Janssen et al. (2006, 2011):

$$t_d \sim Ca^{3/2}$$

Leal et al. (2004, 2007):

$$t_d \sim Ca^{4/3}$$

However…

Note: $Ca = m_2 U_\infty Oh$

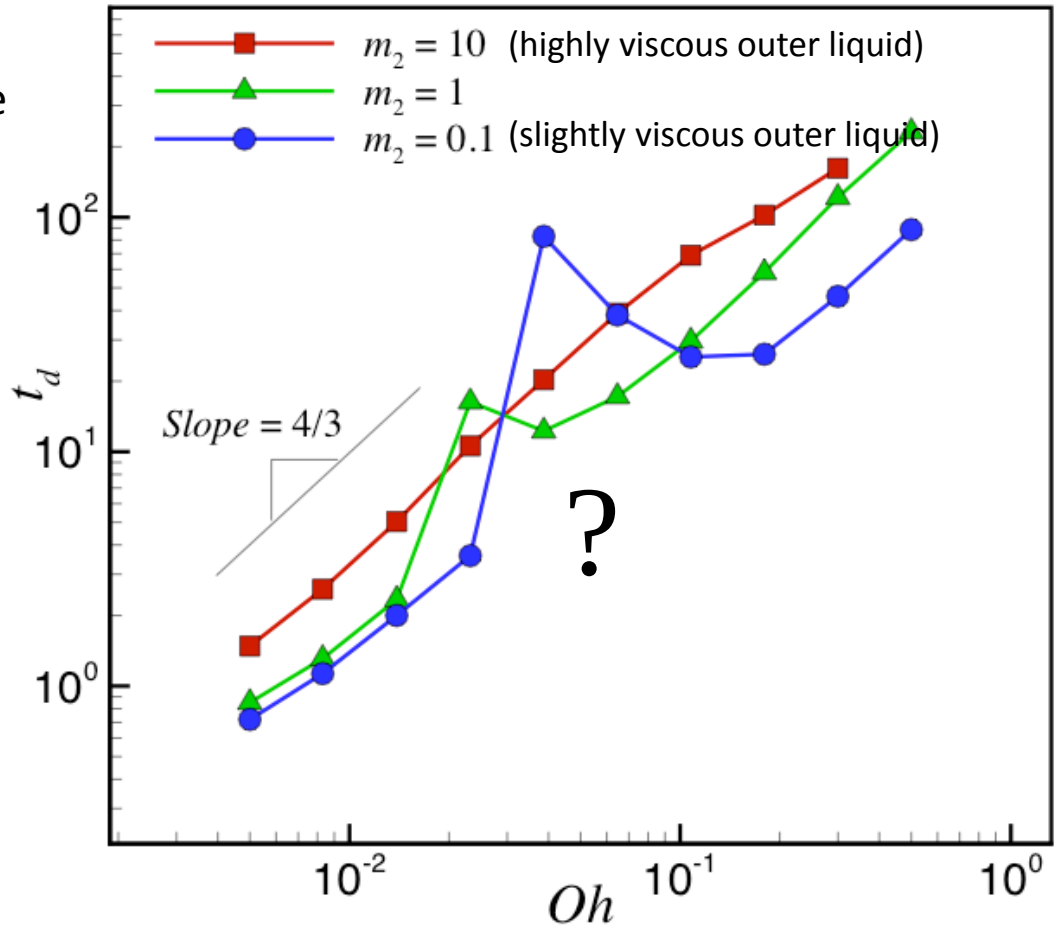

High–intermediate *Oh* systems

$m_2 = 1,\ U_\infty = 0.05,\ A^* = 10^{-10},\ d_2 = 1$

$Oh = 0.108$

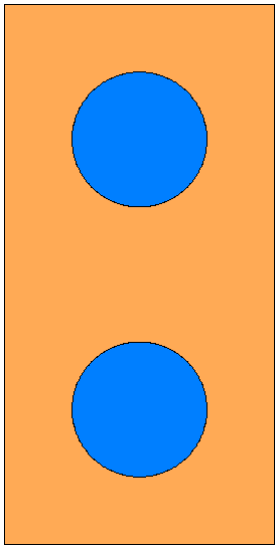

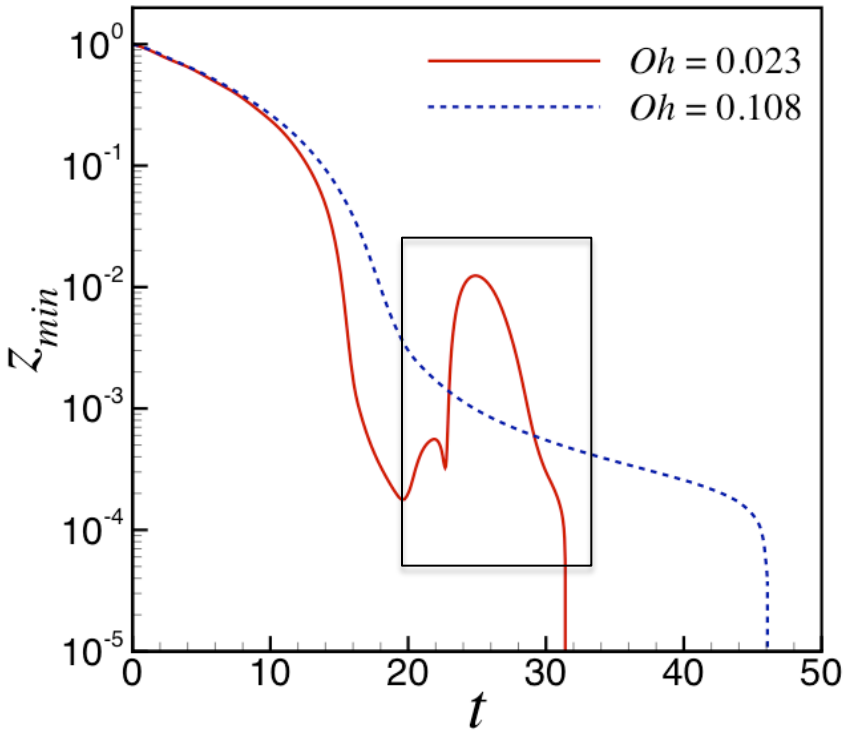

$Oh = 0.023$

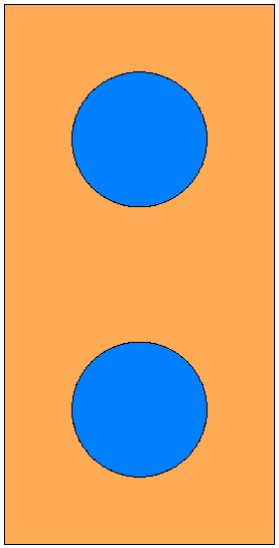

- The rebound effect is observed for intermediate values of *Oh*
- The lower the value of *Oh*, the stronger the inertial effects

Intermediate–low *Oh* systems

$m_2 = 1,\ U_\infty = 0.05,\ A^* = 10^{-10},\ d_2 = 1$

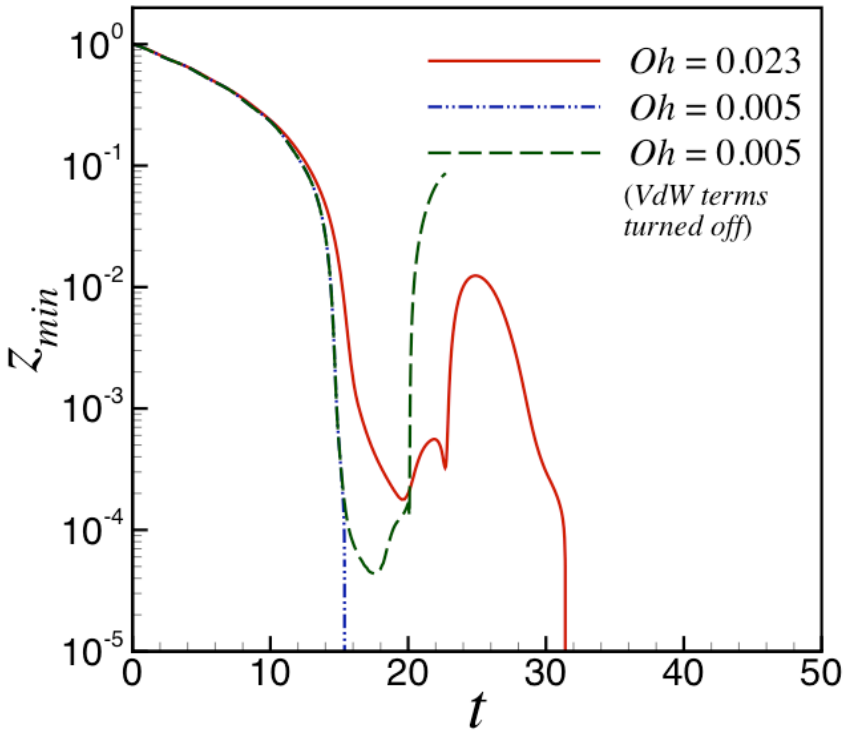

- Van der Waals forces between the droplets become important if they can get sufficiently close to one another before they can bounce off each other

Impact on drainage time

Defined as:

Beginning at

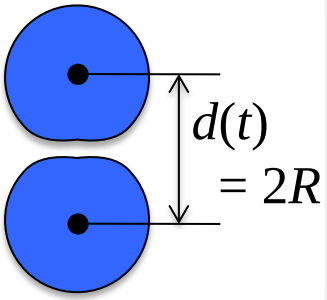

Ending with

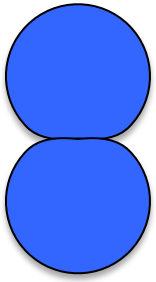

Coalescence

$$Oh = 0.023,\ U_\infty = 0.05,\ d_2 = 1,\ m_2 = 1,\ A^* = 10^{-10}$$

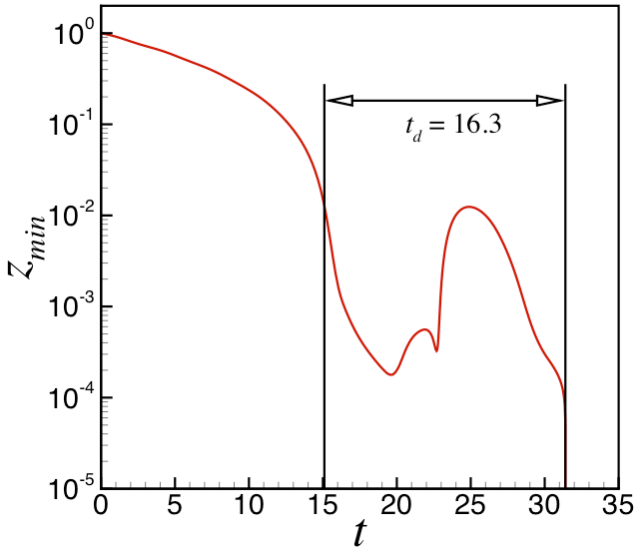

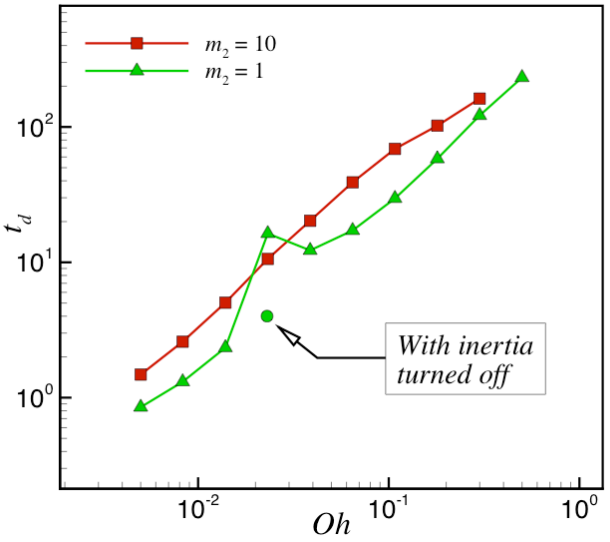

- ***Inertia*** causes the droplets to rebound on first approach at intermediate values of *Oh* resulting in the non-monotonic variation of drainage time with *Oh*
- Accurate prediction/knowledge of drainage time is essential if the results of simulations are to be used in engineering calculations (e.g. population balances) and in engineering design

Conclusions and future work

- High-accuracy, high-resolution simulations have revealed and quantified unexpected role of inertia on drainage and coalescence times in drop coalescence as a function of Ohnesorge number
- At the urging of several industry colleagues, we have extended this work to simulate the coalescence of bubbles (Vishrut Garg et al., presentation made at APS/DFD Conference in November 2017 in Denver, Colorado)
- Also of interest are collisions of drops and bubbles with solid walls (e.g. as in engines) and fluid interfaces
- As warm-up, we have also studied the effects of surfactants on the post-coalescence problem (we will spend 5 minutes on this topic)
- *The main goal for the next year is to analyze through simulations the pre-coalescence problem in the presence of surfactants*

Why is bubble coalescence important?

High viscosity oil-gas systems:

- When a saturated or over-saturated oil is depressurized (e.g., as it goes through a separator), gas bubbles evolve. It is desired that they rise up and leave the oil phase before oil exits the separator. Coalescence of gas bubbles with other bubbles and with a bulk gas phase (at the oil-gas interface) would be an important factor in determining the success of oil-gas separations.

Foam stability/instability:

- Although foams are everywhere, foams of varying quality (or gas volume fraction) are used to "clean" or "sweep" a pipeline of debris. It is important that foams stay foams while flowing and bubble coalescence plays a part in determining that. Also, after sweeping, foams have to be "killed" or separated into gas and liquid; bubble coalescence plays a part in that too.

POST-COALESCENCE OF SURFACTANT-LADEN DROPS

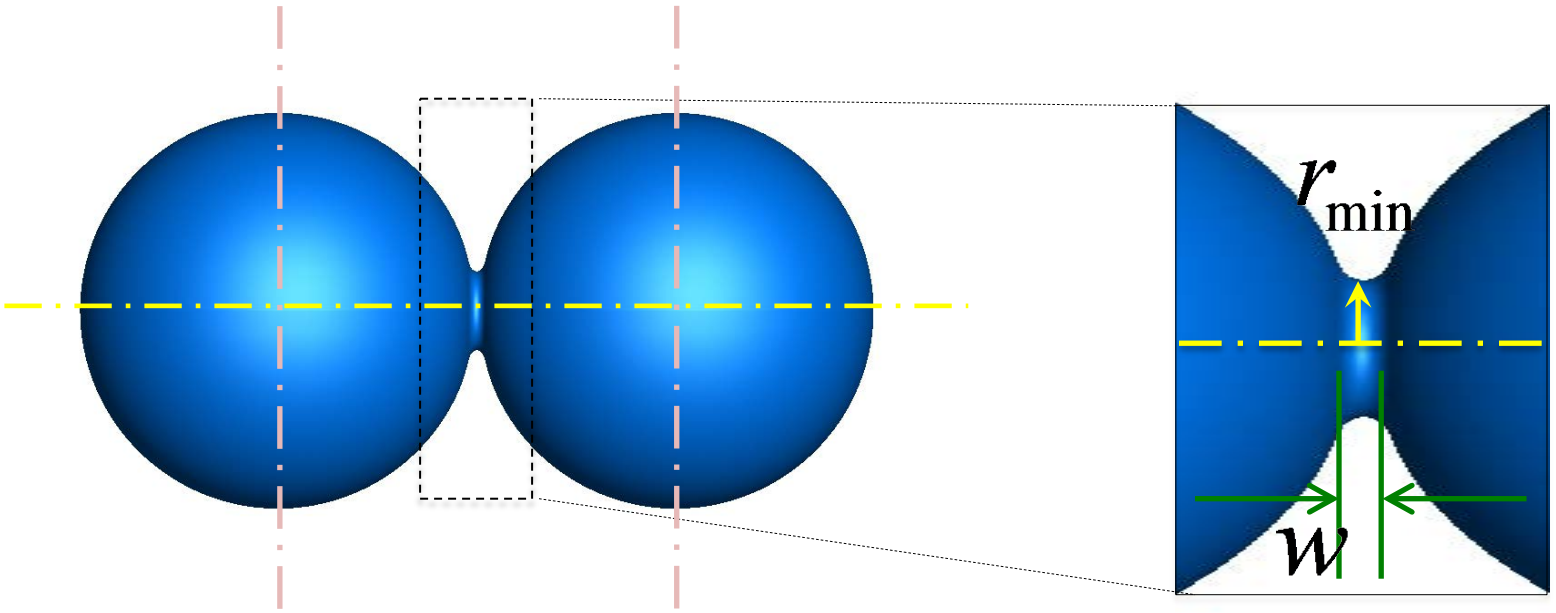

Objectives

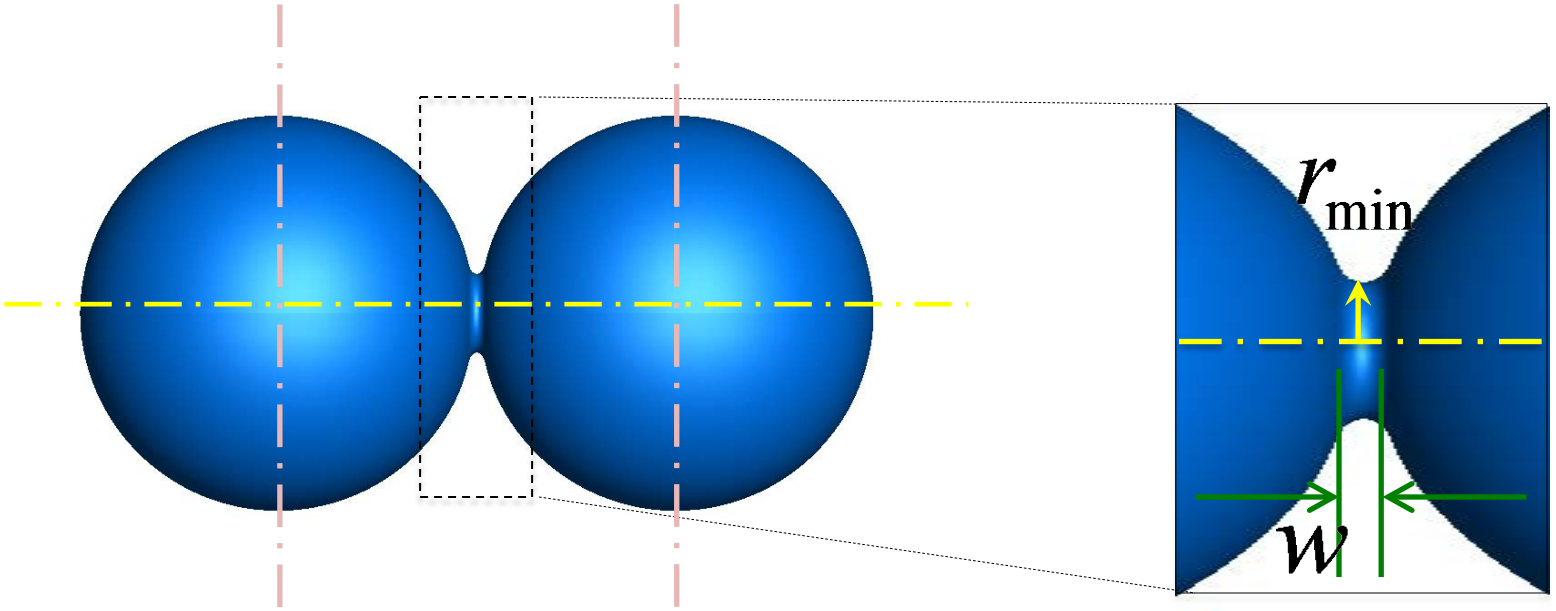

Goal: Elucidate the dynamics that occurs after the two drops have just touched and begin to merge into one drop

Central issue: How does the initially microscopic bridge connecting the two drops expand and grow in time?

Previous work: Conventional understanding

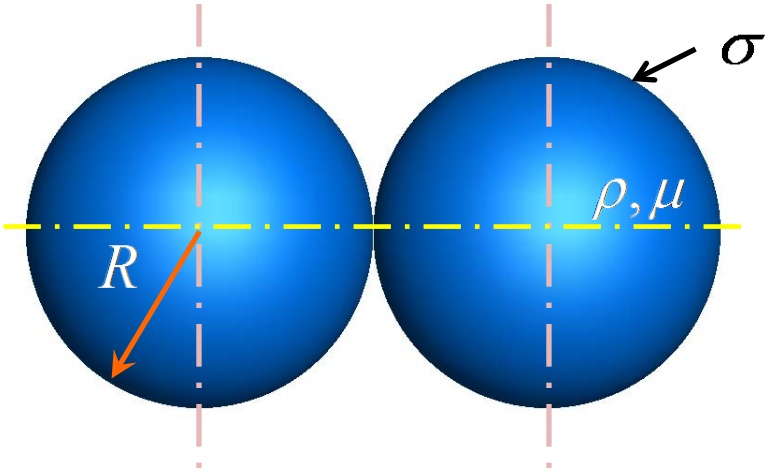

$$Oh = \frac{\mu}{\sqrt{\rho R \sigma}}$$

- Eggers et al. (1999)
  - Stokes regime, S
  - Balance capillary and viscous effects

$$\left(r_{\min} \sim t \log t\right)$$

- Duchemin et al. (2003)
  - Inertial regime, I
  - Balance inertial and capillary forces

$$\left(r_{\min} \sim t^{1/2}\right)$$

$r_{\min} / R$

Phase diagram taken from Paulsen, PRE, 2013

Previous work: Corrected phase diagram

$$Oh = \frac{\mu}{\sqrt{\rho R \sigma}}$$

$$r_{\min} \sim t$$

$$r_{\min} / R$$

❖Paulsen et al.*

- *Inertially-limited-viscous regime, ILV*
- Balance all three effects viz. inertial, viscous and capillary

*Paulsen, J. D., Burton, J. C., Nagel, S. R., Appathurai, S., Harris, M. T., & Basaran, O. A. (2012). The inexorable resistance of inertia determines the initial regime of drop coalescence. Proceedings of the National Academy of Sciences, 109(18), 6857-6861.

Coalescence: Analogy with drop breakup

For a thinning filament

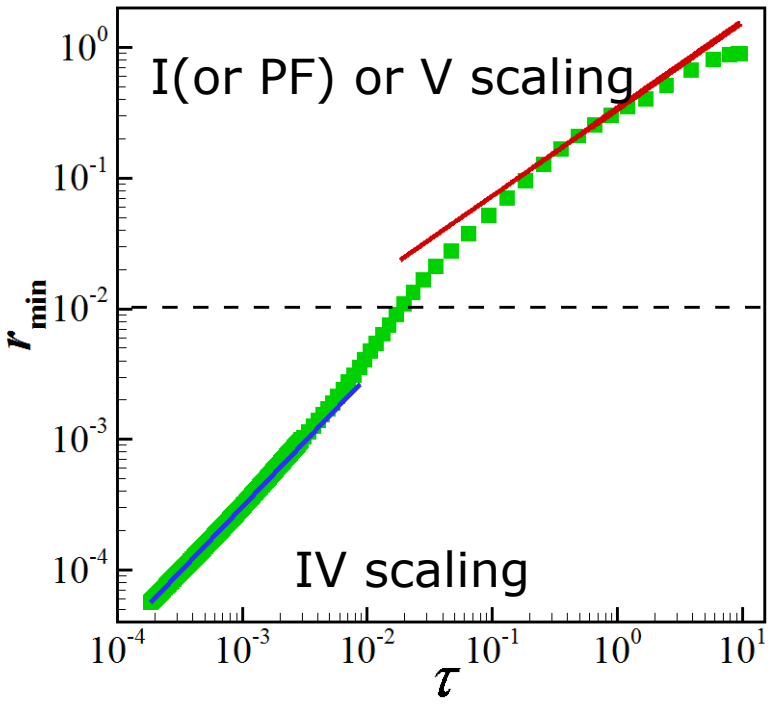

- Singularity due to *out-of-plane curvature* as breakup is approached

  τ is time until breakup

Day R., Hinch J., Lister J., 1998, PRL
Chen Y., Steen P., 1997, JFM
Keller J., Miksis M., 1983, SIAM

Papageorgiou D., 1995, PoF
Eggers J., 1993, PRL
Chen, Notz, Basaran, 2002, PRL

For coalescing drops

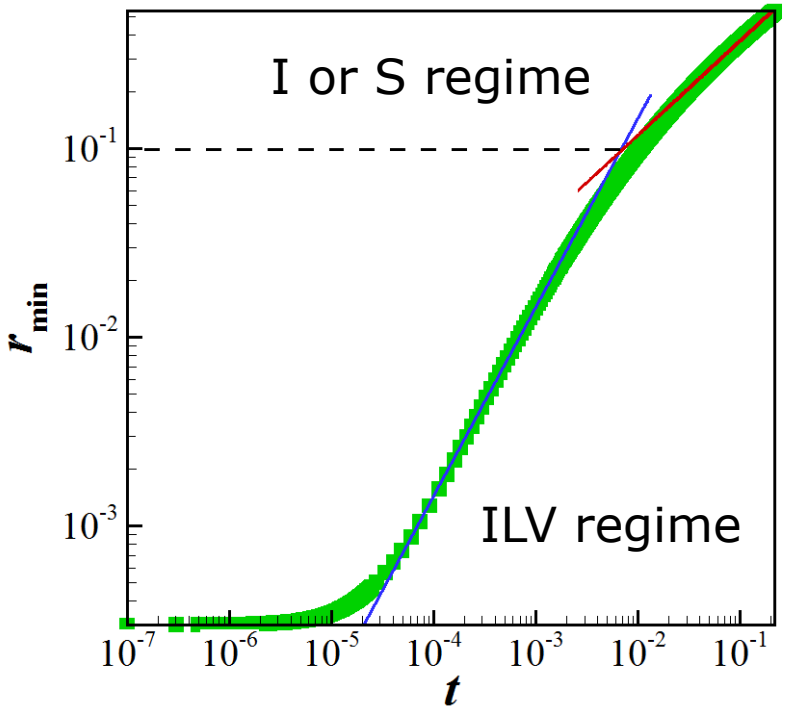

- Singularity due to *in-plane curvature* at the incipience of coalescence

System under consideration

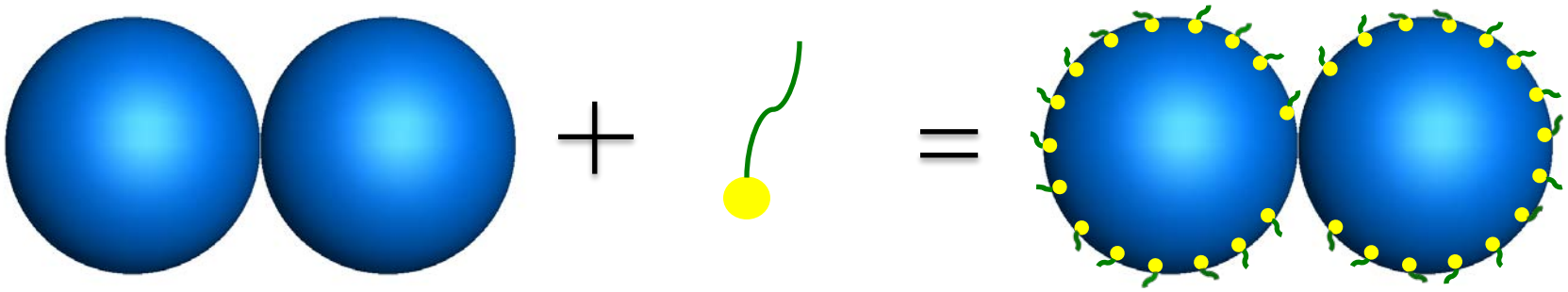

Newtonian drops

Insoluble surfactant

Drops covered with surfactant

Liao, Y. C., Franses, E. I., & Basaran, O. A. (2006). Deformation and breakup of a stretching liquid bridge covered with an insoluble surfactant monolayer. Physics of Fluids, 18(2), 022101.

Problem setup and non-dimensionalization

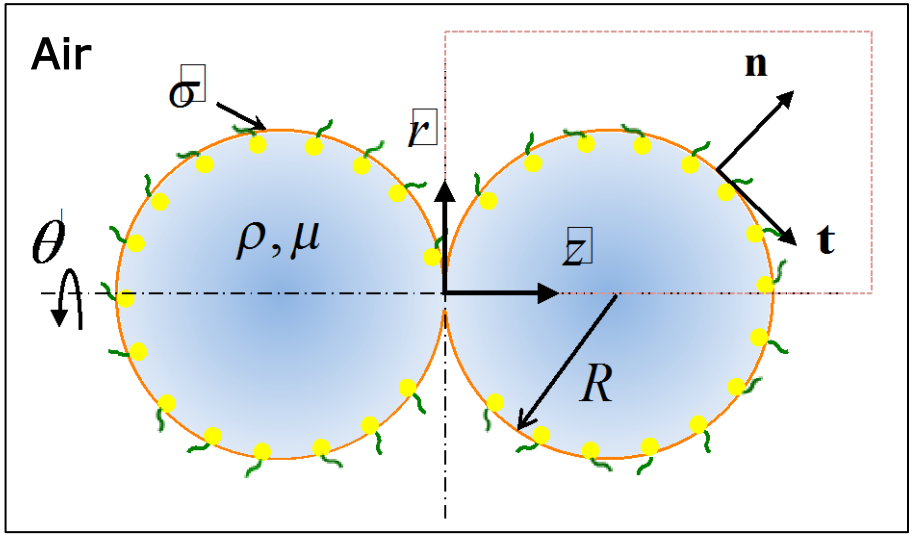

Characteristic scales:

$$t_c = \sqrt{\frac{\rho R^3}{\sigma_0}} \qquad p_c = \frac{\sigma_0}{R}$$
$$l_c = R \qquad \sigma_c = \sigma_0$$
$$v_c = \frac{l_c}{t_c} \qquad \Gamma_c = \Gamma_m$$

Dimensionless groups:

	Values considered	Typical values
$Oh \equiv \frac{\mu}{\sqrt{\rho R \sigma_0}}$	0.1	10^{-3} to 10
$Pe \equiv \frac{R^2}{D_s t_c}$	10 to 10^3	10^3 to 10^4

	Values considered	Typical values
$\beta \equiv \frac{\Gamma_m \tilde{R} T}{\sigma_0}$	0.3	≤ 0.3
$\Gamma_0 \equiv \frac{\tilde{\Gamma}_0}{\Gamma_m}$	0.1	$\mathcal{O}(0.1)$

Mathematical formulation

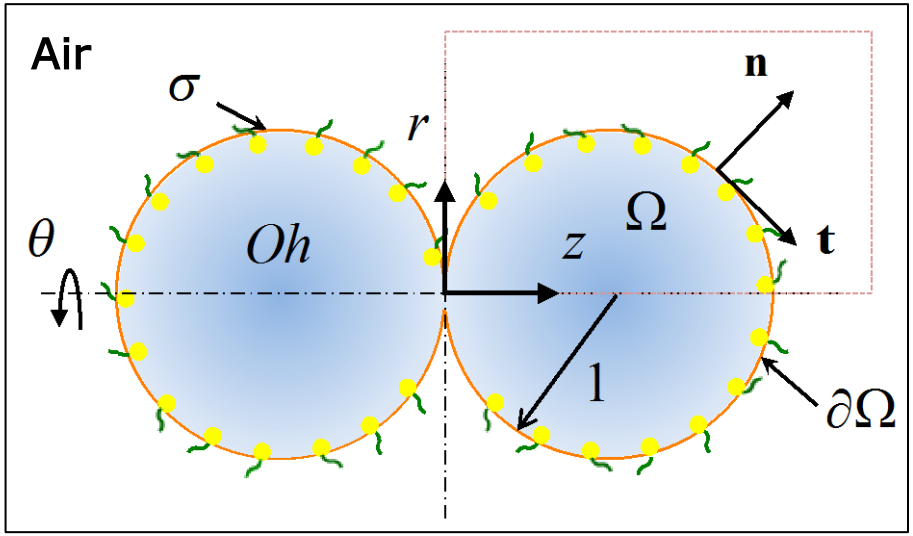

Navier-Stokes system:

$$\nabla \cdot \mathbf{v} = 0$$

$$\frac{\partial \mathbf{v}}{\partial t} + \mathbf{v} \cdot \nabla \mathbf{v} = \nabla \cdot \mathbf{T}$$

where,

$$\mathbf{T} = -p\mathbf{I} + Oh\left((\nabla \mathbf{v}) + (\nabla \mathbf{v})^T\right)$$

$$\mathbf{v} = u\mathbf{e}_r + v\mathbf{e}_z$$

Ω

Surfactant transport and surface tension variation:

$$\frac{\partial \Gamma}{\partial t} + \nabla_s \cdot (\mathbf{v}\Gamma) = \frac{1}{Pe}\nabla_s{}^2\Gamma$$

$$\sigma = 1 + \beta \ln(1 - \Gamma)$$

$$\Gamma(t = 0) = 0.1$$

$\partial\Omega$

Free surface boundary conditions:

$$\mathbf{n} \cdot (\mathbf{v} - \mathbf{v_S}) = 0$$

$$\mathbf{n} \cdot \mathbf{T} = -2H\sigma\mathbf{n} + \nabla_s \sigma$$

$\partial\Omega$

Coalescence of drops without surfactants

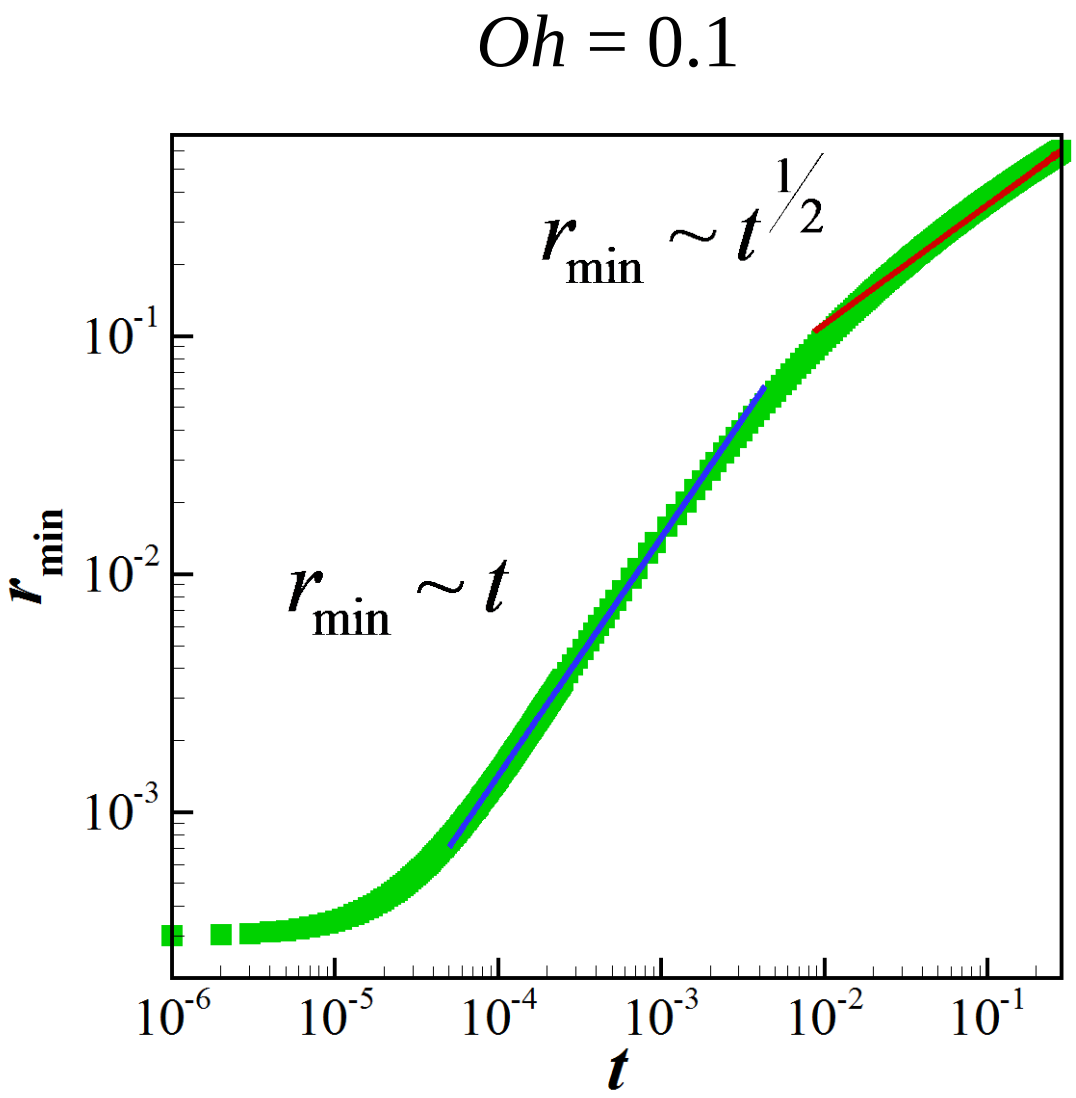

ILV → I

Coalescence of drops with surfactants

$Oh = 0.1$, $Pe = 10$

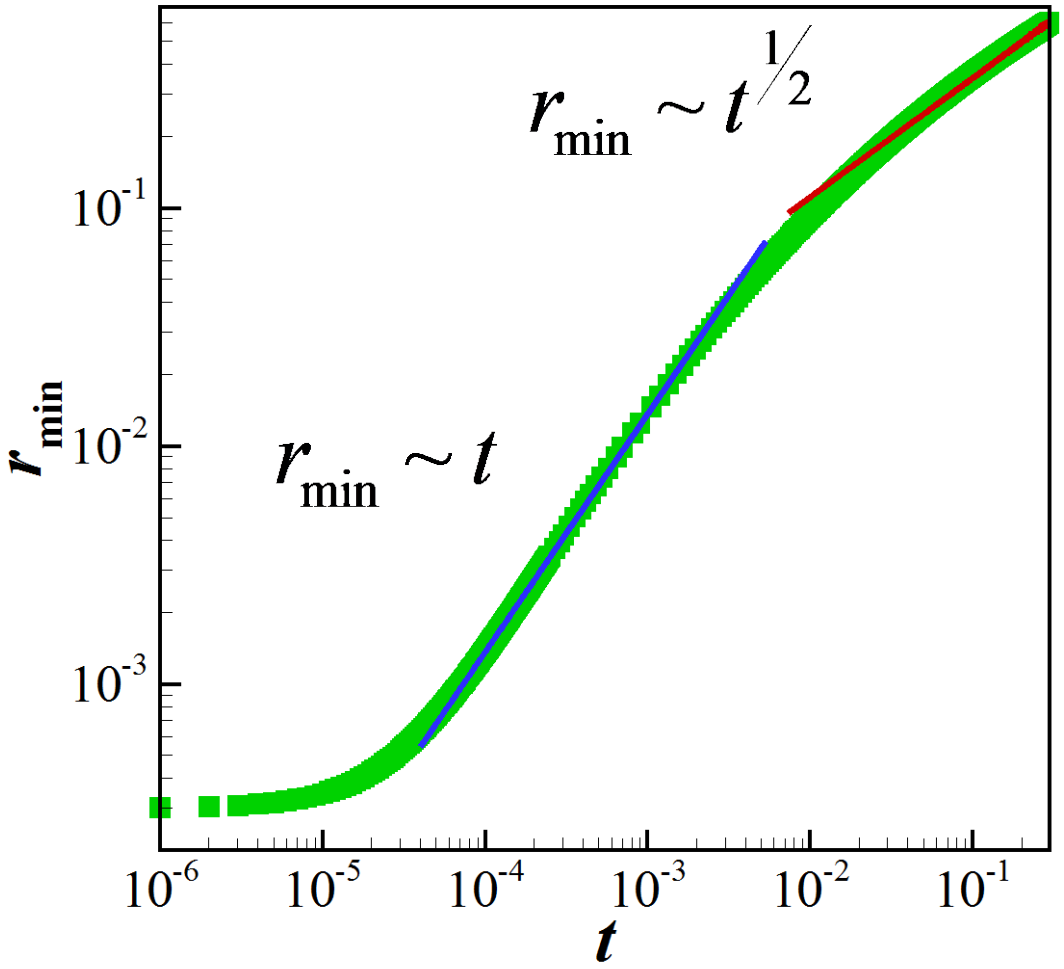

ILV → I

Same as before

Coalescence of drops with surfactants (contd.)

$Oh = 0.1$, $Pe = 150$

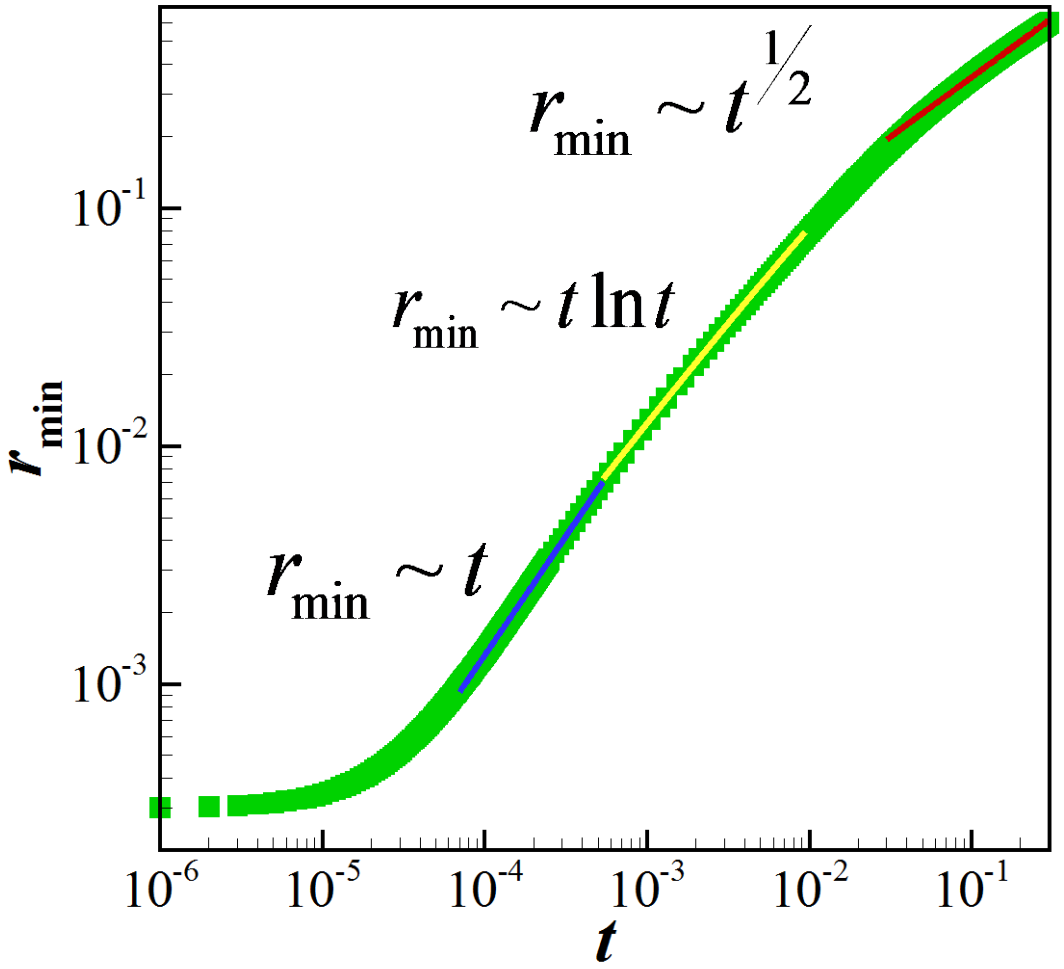

ILV → IR → I

New intermediate regime (IR)

What happens when we increase Pe?

$Pe = 150$

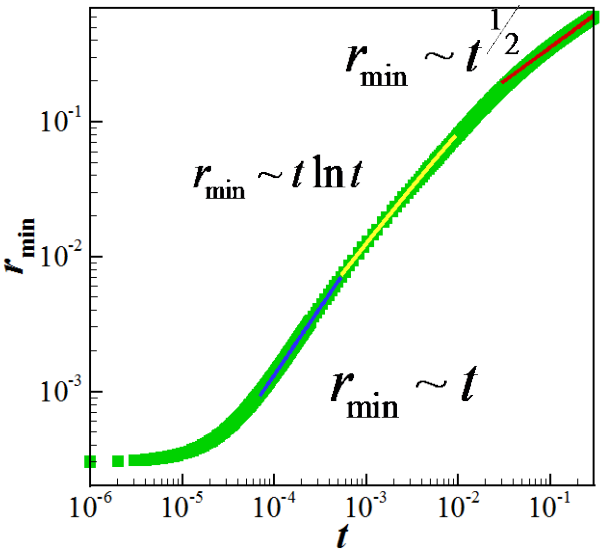

ILV → IR → I

$Pe = 300$

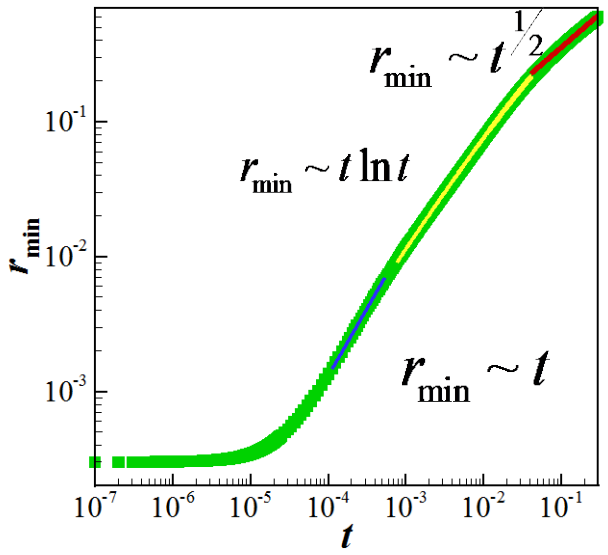

ILV → IR → I

$Pe = 1000$

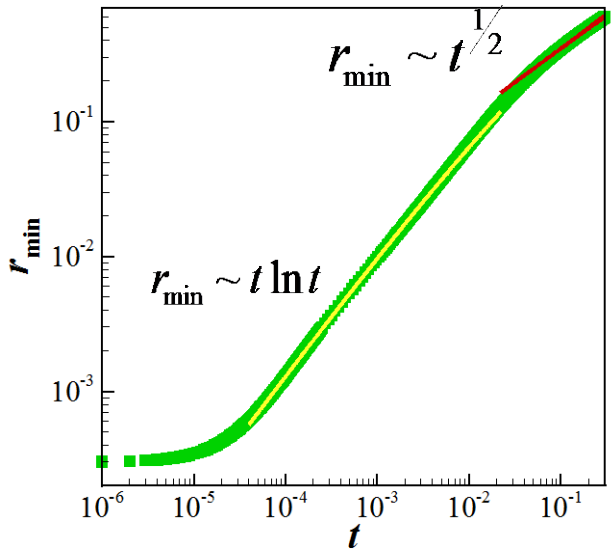

ILV → IR → I

As, Pe ↑ *IR* ↑ *ILV* ↓

How do surfactants migrate at different Pe?

Small Pe (=10)

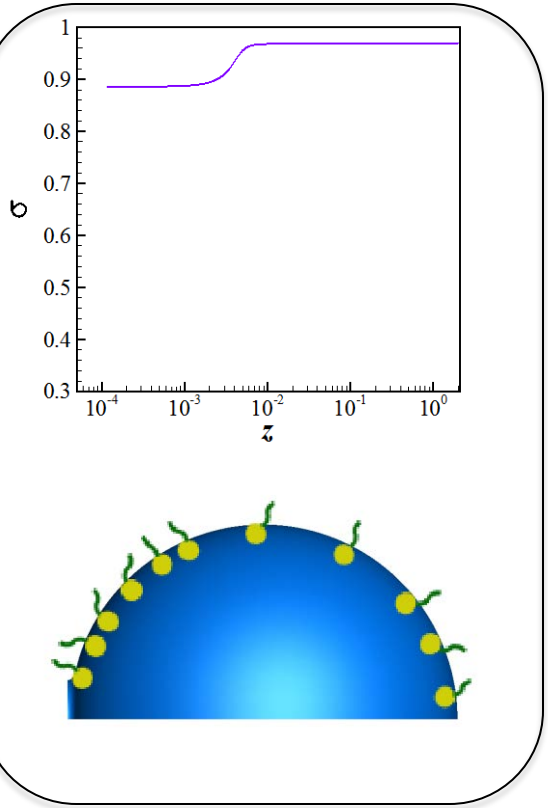

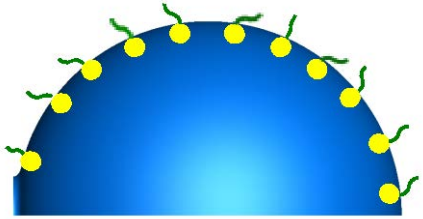

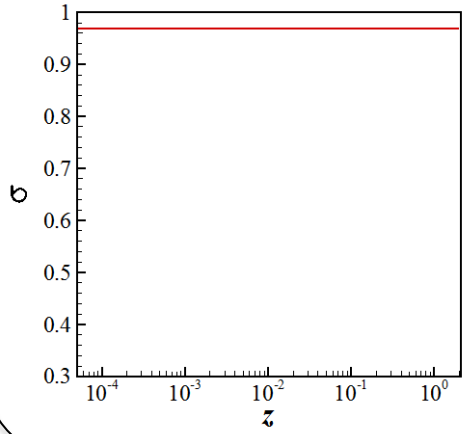

Large Pe (= 300)

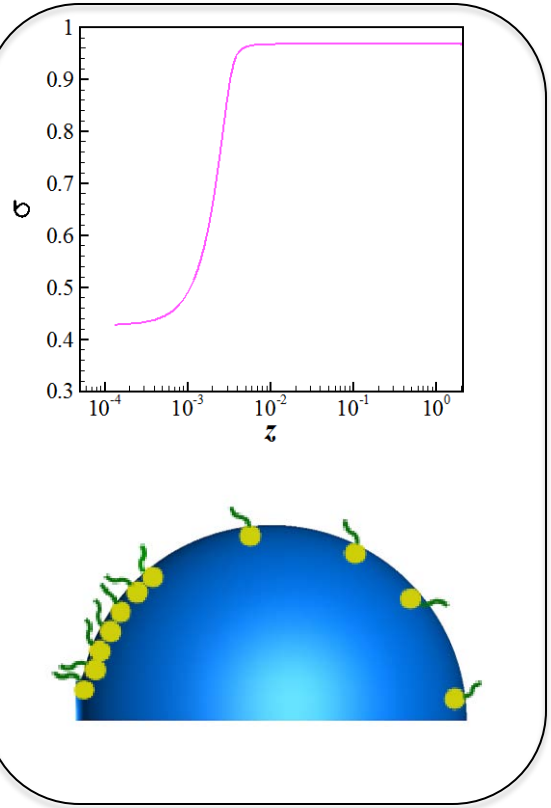

What happens when $Pe = 300$?

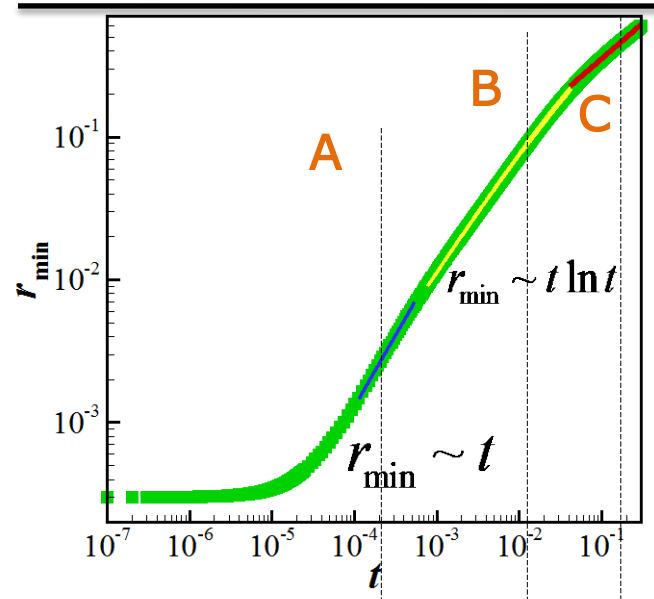

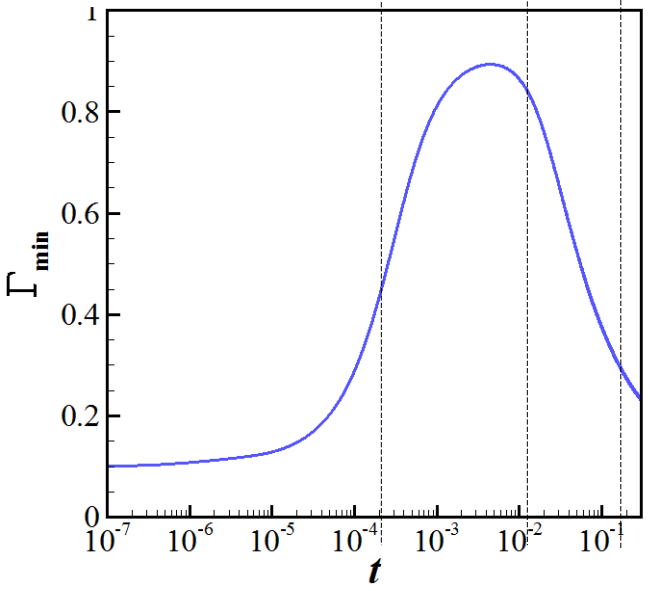

$r_{min} \sim t^{1/2}$

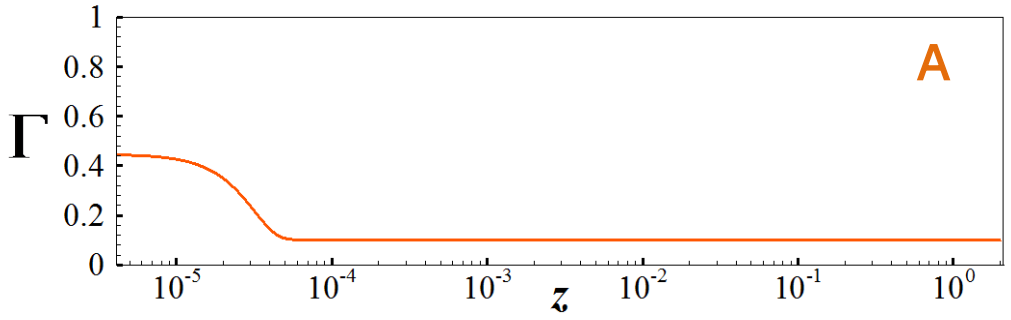

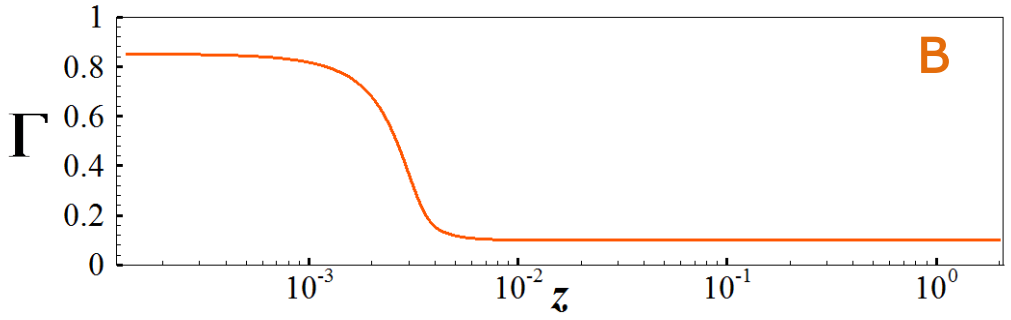

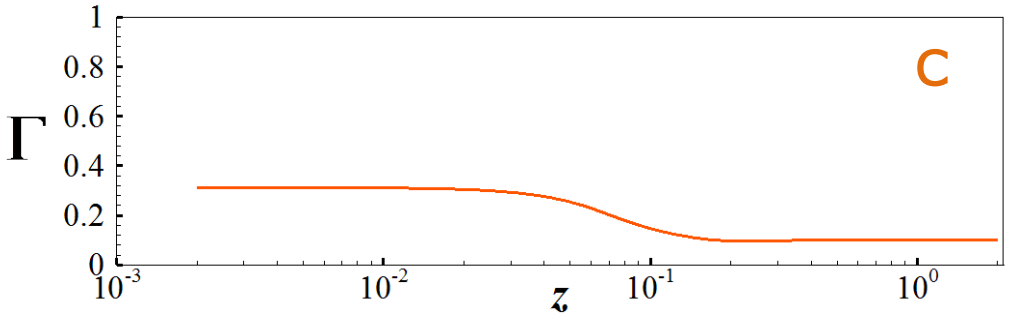

Summary and conclusions